Breathless through Time: Oxygen and Animals across Earth's History

Erik A. Sperling[1,*], Thomas H. Boag[2], Murray I. Duncan[1,3], Cecilia R. Endriga[1], J. Andres Marquez[1], Daniel B. Mills[1,4], Pedro M. Monarrez[1], Judith A. Sclafani[5], Richard G. Stockey[1], and Jonathan L. Payne[1]

[1] Department of Geological Sciences, Stanford University, Stanford, California 94305
[2] Department of Earth and Planetary Sciences, Yale University, New Haven, Connecticut 06520
[3] Hopkins Marine Station, Stanford University, Pacific Grove, California 93950
[4] Penn State Extraterrestrial Intelligence Center, Pennsylvania State University, University Park, Pennsylvania 16802
[5] Department of Earth and Planetary Sciences, University of California, Davis, Davis, California 95616

Abstract

Oxygen levels in the atmosphere and ocean have changed dramatically over Earth history, with major impacts on marine life. Because the early part of Earth's history lacked both atmospheric oxygen and animals, a persistent co-evolutionary narrative has developed linking oxygen change with changes in animal diversity. Although it was long believed that oxygen rose to essentially modern levels around the Cambrian period, a more muted increase is now believed likely. Thus, if oxygen increase facilitated the Cambrian explosion, it did so by crossing critical ecological thresholds at low O_2. Atmospheric oxygen likely remained at low or moderate levels through the early Paleozoic era, and this likely contributed to high metazoan extinction rates until oxygen finally rose to modern levels in the later Paleozoic. After this point, ocean deoxygenation (and marine mass extinctions) is increasingly linked to large igneous province eruptions—massive volcanic carbon inputs to the Earth system that caused global warming, ocean acidification, and oxygen loss. Although the timescales of these ancient events limit their utility as exact analogs for modern anthropogenic global change, the clear message from the geologic record is that large and rapid CO_2 injections into the Earth system consistently cause the same deadly trio of stressors that are observed today. The next frontier in understanding the impact of oxygen changes (or, more broadly, temperature-dependent hypoxia) in deep time requires approaches from ecophysiology that will help conservation biologists better calibrate the response of the biosphere at large taxonomic, spatial, and temporal scales.

Introduction

Because oxygen is a fundamental requirement for animal life and because oxygen levels in the ocean-atmosphere system have clearly changed over Earth history, the availability of oxygen has come to be regarded by many geologists and paleontologists as a master variable governing animal diversity through time. Understanding the relationship between oxygen and animal evolution is critical to understanding the rise and trajectory of complex life on Earth, and it also bears important lessons for modern and future global change. The fossil record offers valuable opportunities to investigate biotic responses to changes in Earth's climate because these responses are not skewed by human interference (*i.e.*, overexploitation or habitat loss), span a greater temporal scale

Received 8 February 2022; Accepted 30 June 2022; Published online 23 September 2022.
* Corresponding author: esper@stanford.edu.
Abbreviations: Φ, metabolic index; A_o, an organism's hypoxia tolerance; E_o, representation of how hypoxia tolerance changes with temperature; GOE, Great Oxidation Event; kyr, thousand years; LIP, large igneous province; Ma, million years ago; MIF-S, mass-independent fractionation of sulfur isotopes; *n*, allometric scaling of an organism's oxygen supply and demand balance with its body size; OMZ, oxygen minimum zone; % PAL, percentage of present atmospheric level; PETM, Paleocene-Eocene Thermal Maximum extinction; pO_2, partial pressure of oxygen; SMR, standard metabolic rate.

The Biological Bulletin, October 2022, volume 243, number 2: 000–000. https://doi.org/10.1086/721754

than can be studied in laboratory experiments, and represent our only source of data on actual outcomes of changes in climate-related stressors (Harnik *et al.*, 2012; Calosi *et al.*, 2019; Clapham, 2019). Most critically, the fossil record is our only source of data for understanding whether most species' extinctions are driven by physiological or ecological processes. Although physiological stressors (*e.g.*, temperature-dependent hypoxia, ocean acidification) are the pertinent environmental factors for marine organisms, it is an open question whether most species-level extinction has occurred or will occur as a direct result of these stressors or *via* physiologically driven stress on keystone species, followed by trophic cascades and ecologically driven extinction for other species. The main challenge in learning and applying these lessons is moving beyond parallel and correlative studies of the fossil record and the geochemical record of ancient oceans. This is ultimately necessary if we are to ask questions such as how extinction selectivity during ancient hypoxic events corresponds to phylogeny, biogeography, or functional morphology, or whether extinction is likely to be mediated directly by physiology or ecological cascades. The answers to such questions will sharpen our ability to use the geologic record to predict biological responses in the future warming and deoxygenating ocean.

In this article, we first aim to provide an accessible introduction to how geochemists track redox changes in ancient oceans (which ultimately leads to inferences of global oceanic and atmospheric oxygen). Next, we review current knowledge of Earth's oxygen history, moving from the anoxic oceans and atmospheres of the Archean eon (4.0–2.5 billion years ago) to the modern well-oxygenated state, where deoxygenation (and global warming) is largely driven by massive carbon inputs from large igneous province (LIP) super-eruptions (Fig. 1). We then discuss how animals evolved and responded to oxygen changes throughout this history, particularly aiming to use ecological space-for-time substitutions and modern ecophysiological approaches to link environmental change with biotic responses. We argue that such approaches have high promise for attaining more mechanistic understanding of how oxygen changes affected animals across timescales. Considering the past ~400 million years of Earth history, we emphasize the role of LIPs in driving low-oxygen events in the ocean. We specifically dissect the evidence for environmental change resulting from the eruption of the Siberian Traps LIP, which caused the most devastating mass extinction in Earth's history at the Permian-Triassic boundary. Finally, we discuss the lessons for modern anthropogenic global change that can be drawn from ancient low-oxygen oceans, as well as highlight future research directions that will help build on our current knowledge.

Reading the Record of Oxygen in Earth's Past

When discussing atmospheric oxygen in Earth's past, geologists and modelers commonly describe these levels by using

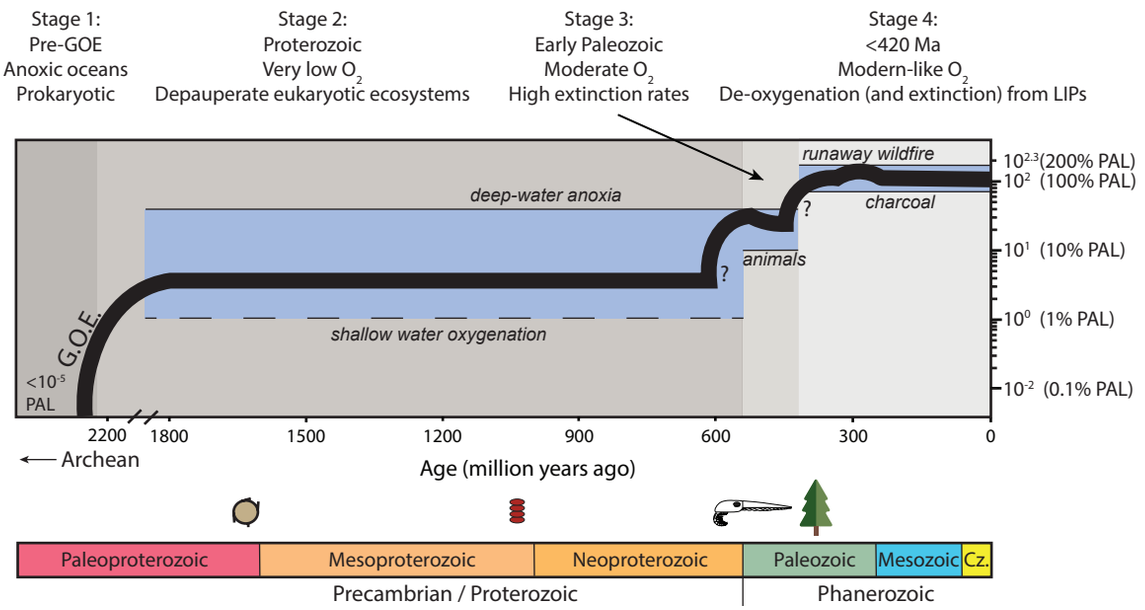

Figure 1. The four broad stages of atmospheric oxygen and life through Earth history, with oxygen in log scale as percent of present atmospheric levels (% PAL). Shown is the best-guess estimate of atmospheric oxygen (thick black line) and geochemical and biologic constraints detailed in the main text (thin black lines bounding blue permissive O_2 state space). It is known with certainty that the Earth irreversibly transitioned from an essentially anoxic ocean-atmosphere system to an oxic state ~2200 million years ago (note the break in scale at 1800 Ma). Although the timing, magnitude, and number of increases are not clear, it is likely that atmospheric oxygen rose near the Neoproterozoic-Paleozoic boundary and in the mid-Paleozoic. Shown above the geologic timescale are major evolutionary events; from left to right, these are the first total-group eukaryotic fossils (~1600 Ma), the first crown-group eukaryotic fossils (~1050 Ma), the first animals near the end of the Neoproterozoic (~570 Ma), and the first trees in the mid-Paleozoic. Cz., Cenozoic; G.O.E., Great Oxidation Event; LIP, large igneous province.

percentage of present atmospheric level (% PAL; present = 100%). For marine redox state or dissolved oxygen levels in ancient oceans, geologists commonly use a descriptive scheme that differs slightly from that currently in use in modern global change studies. First, anoxic conditions are recognized to be either "euxinic," with free sulfide, or "ferruginous," with free ferrous iron, at least enough to titrate out available sulfide (Poulton and Canfield, 2011). In contrast to modern anoxic settings, which are almost all euxinic, it is now recognized that, especially in the Proterozoic and early Paleozoic (~2000 to 400 million years ago [Ma]), most anoxic settings were ferruginous (Canfield *et al.*, 2008; Planavsky *et al.*, 2011; Guilbaud *et al.*, 2015; Sperling *et al.*, 2015b, 2021). Similar to modern global change biologists, geologists use the term "suboxic" to refer to the feather edge of anoxia, where very few animals aside from chemosynthetic organisms can live. Here, we define suboxic as ~1.5% air saturation, ~5 μmol L^{-1}, ~0.1 mL L^{-1} O_2 (note that oxygen concentrations expressed in μmol L^{-1} or mL L^{-1} will be dependent on temperature, pressure, and salinity; Hofmann *et al.*, 2011). In contrast to global change biologists, geologists and paleontologists commonly use the term "dysoxic" instead of "hypoxic" to define oxygen levels between suboxic and fully oxic. In our opinion, using the term hypoxic, which is a species- or organism-specific physiological state, to define the geochemical characteristics of a water mass is incongruent. Further, a main point of this paper is understanding the combined effects of changing oxygen and temperature. Because hypoxia is the synergistic interaction of these two environmental parameters (*e.g.*, Deutsch *et al.*, 2015), even for a single organism a water parcel can be hypoxic (or not) across a range of oxygen levels, depending on the temperature. Thus, we will use dysoxic in this paper to describe low-oxygen conditions and define it as O_2 levels between suboxia (less than ~1.5% air saturation) and normoxia (greater than ~31% air saturation, >88 μmol L^{-1}, >2 mL L^{-1} O_2). Sperling *et al.* (2015a) and Cole *et al.* (2020) have recently reviewed oxygen nomenclature across and within fields in geology and modern biology and oceanography.

For studies of the Holocene (the past 12,000 years) or Pleistocene (the past 2.6 million years), geologists are able to utilize small bubbles of ancient air trapped in ice cores. This has allowed for direct measurement of atmospheric chemistry, most notably the dramatic changes in CO_2 related to orbitally forced climate cycles (*e.g.*, Petit *et al.*, 1999) but also atmospheric O_2 (Yan *et al.*, 2021). For deeper Earth history, however, atmospheric oxygen or marine redox changes—with a few exceptions detailed below—must be reconstructed through indirect proxy methods derived from sedimentary archives. Our two major archives for understanding paleoenvironmental conditions on ancient Earth are carbonates (composed of sedimentary minerals, such as calcite, aragonite, and dolomite, that are precipitated from seawater as both inorganic precipitates, such as ooids, and the organic biominerals of organisms, such as corals or bivalves) and shales or mudstones (composed of fine-grained particles that represent the transported remnants of previously weathered rocks). Carbonate proxies tend to rely on the abundance or isotopic ratios of elements that are incorporated as trace constituents into the carbonate crystal lattice, whereas shale proxies generally rely on elements that associate with organic matter or pyrite under reducing conditions. Each of these sedimentary archives can record local proxies, which reveal information about the bottom waters directly above a given sedimentary locality but with no global context, and global proxies, which reveal the mean state in the ocean but with no spatial or bathymetric context (for a comprehensive review of various proxy approaches, see Kendall, 2021). Local proxies for shales include iron speciation (Poulton, 2021) and the enrichment of redox-sensitive trace metals such as molybdenum and uranium (Tribovillard *et al.*, 2012), whereas carbonates can be studied using iodine to calcium (I/Ca) ratios (Lu *et al.*, 2018) or cerium anomalies (Bellefroid *et al.*, 2018; Liu *et al.*, 2021). Critically, I/Ca may be able to fingerprint dysoxic conditions (Lu *et al.*, 2016), in contrast to most local proxies in shales, which can robustly distinguish oxic *versus* euxinic conditions but may have difficulty distinguishing fully oxygenated from dysoxic or ferruginous conditions (discussed by Sperling *et al.*, 2018). The global marine redox landscape can be studied in shales by using molybdenum and uranium isotopes (Kendall *et al.*, 2017; Stockey *et al.*, 2020), which track variations in the extent of anoxic seafloor, or thallium isotopes (Them *et al.*, 2018), which track variations in the extent of oxic seafloor.

In carbonates, the global redox landscape is increasingly studied using uranium isotopes (Fig. 2), which we will focus on here, particularly as they pertain to mass extinction events. Under anoxic conditions in the oceans, the reduction of soluble U(VI) to insoluble U(IV) at the sediment-water interface is associated with an isotopic fractionation because ^{238}U is reduced more rapidly than ^{235}U (due to the nuclear volume effect). Although there can be local differences, the average isotopic offset between seawater and anoxic sediments is about +0.6‰. Thus, expansion of ocean anoxia is expected to cause not only a reduction in ocean uranium concentrations but also a reduction in the oceanic $^{238}U/^{235}U$ ratio (typically reported in delta notation as $\delta^{238}U$; reviewed in Zhang *et al.*, 2020). The long residence time of uranium in seawater (~500 thousand years [kyr]) relative to the ocean mixing time (~1–2 kyr) leads to the oceans being well mixed in terms of the $^{238}U/^{235}U$ ratio, meaning this ratio is the same anywhere in the ocean. Because carbonates trap minute quantities of uranium in their crystal lattice during precipitation with minimal or at least understandable offset from seawater (Chen *et al.*, 2018), and because the ocean is well mixed with respect to uranium, this means that any carbonate deposited in an ancient ocean should be recording the U isotope composition of its seawater. And since the isotopic composition of seawater is primarily set by the ratio between seafloor covered by oxic

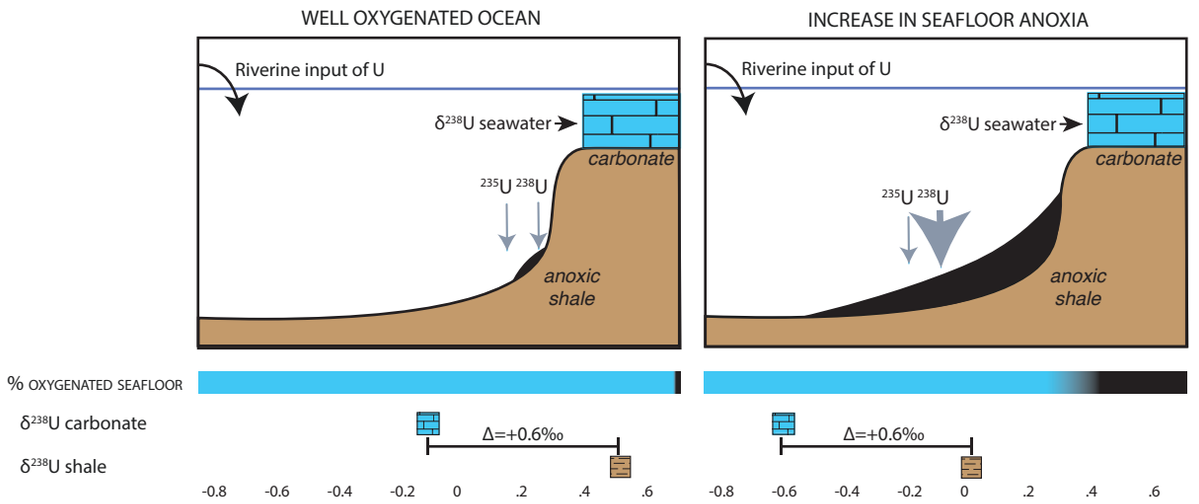

Figure 2. The carbonate uranium proxy is one of the most commonly used global redox proxies in deep time, especially for studying mass extinctions. Riverine U input is broadly constant through time, and the oceanic $^{238}U/^{235}U$ ratio (typically reported as $\delta^{238}U$) is primarily set by the proportion of oxic *versus* anoxic seafloor. Under anoxic bottom waters, the heavier ^{238}U isotope is preferentially reduced (with a fractionation of +0.6‰) and trapped in anoxic shales. Expansion of anoxic seafloor (*i.e.*, right-hand panel) leads to higher burial flux of ^{238}U (gray vertical arrows). Removal of the heavy isotope causes the seawater $\delta^{238}U$ ratio to become lighter (more negative). Seawater uranium is incorporated into shallow-water carbonates with relatively little isotopic offset, and thus, an expansion of anoxic seafloor will be recorded in the rock record as a negative excursion in $\delta^{238}U$ of carbonates (*e.g.*, Fig. 7). See Lau *et al.* (2016) and Zhang *et al.* (2020) for additional details.

versus anoxic bottom waters, geochemists can then quantitatively back-calculate (using increasingly sophisticated modeling techniques) the global redox landscape.

Atmospheric and Marine Oxygen Levels through Earth History

At the broadest level, Earth appears to have experienced four stages of atmospheric oxygen levels. There were likely important oscillations within these stages, especially during the middle part of Earth's history; but from the perspective of changes that were relevant to animal life in the oceans, these stages are the early part of Earth history in the Archean and early Paleoproterozoic (~4000–2200 Ma; when the oceans and atmosphere were anoxic), the mid-Proterozoic (~2200–540 Ma; when oxygen was stably present but at relatively low levels, perhaps 1%–10% of present levels), the early Paleozoic (~540–420 Ma; when oxygen levels were perhaps 10%–40% of present levels), and the later Paleozoic to present (~420 Ma to present; when atmospheric oxygen was similar to present) (Figs. 1, 3). Despite the considerable study into the question of atmospheric oxygen through time and general agreement on the broad history, geologists and geochemists can recognize only two absolute values with clarity and a lack of controversy. Photochemical reactions in the atmosphere between incoming UV and SO_2 generate sulfur compounds wherein the sulfur isotopes are fractionated in a manner independent of their mass (mass-independent fractionation [MIF-S]). Such reactions occur today; but in the presence of even minute amounts of atmospheric oxygen, as low as 0.001% PAL (10^{-5} PAL), the products of these atmospheric reactions are oxidized and pass through the oceanic sulfur cycle, and any mass-independent fractionation effects are erased (Pavlov and Kasting, 2002). The MIF-S signals are recorded in the Archean and early Paleoproterozoic sulfur record (first discovered by Farquhar *et al.*, 2000), providing an unambiguous signal of an essentially anoxic atmosphere on early Earth. The MIF-S then disappears, marking the Great Oxidation Event, or GOE. Current controversies include the timing of oxygenation (and whether it was protracted or sudden; Poulton *et al.*, 2021; Hodgskiss and Sperling, 2022), but MIF-S and other markers of an anoxic atmosphere never return after ~2.2 billion years ago, marking the irreversible oxygenation of Earth's atmosphere.

The second unambiguous constraint on atmospheric oxygen concentration comes from the fossil record of charcoal (burned plant material). A series of elegant calculations and experiments have demonstrated that plant material will not ignite without ~15% O_2 in the atmosphere (by volume, equivalent to 73% PAL, given 21% O_2 by volume in the atmosphere today), and globally distributed runaway wildfires will occur at greater than ~35% O_2 (=170% PAL) (Jones and Chaloner, 1991; Wildman *et al.*, 2004; Belcher and McElwain, 2008). Note, however, that this upper bound has not been experimentally determined with certainty and that many commonly cited secondary sources in the literature (*e.g.*, Kump, 2008) cite earlier studies on paper ignition (Watson *et al.*, 1978) that are not realistic for natural fuels (Wildman *et al.*, 2004). Nonetheless, the presence of both charcoal and unignited plant fossils in the rock record since the late Silurian (~420 million years ago) has allowed geologists to robustly infer that atmospheric oxygen has been between

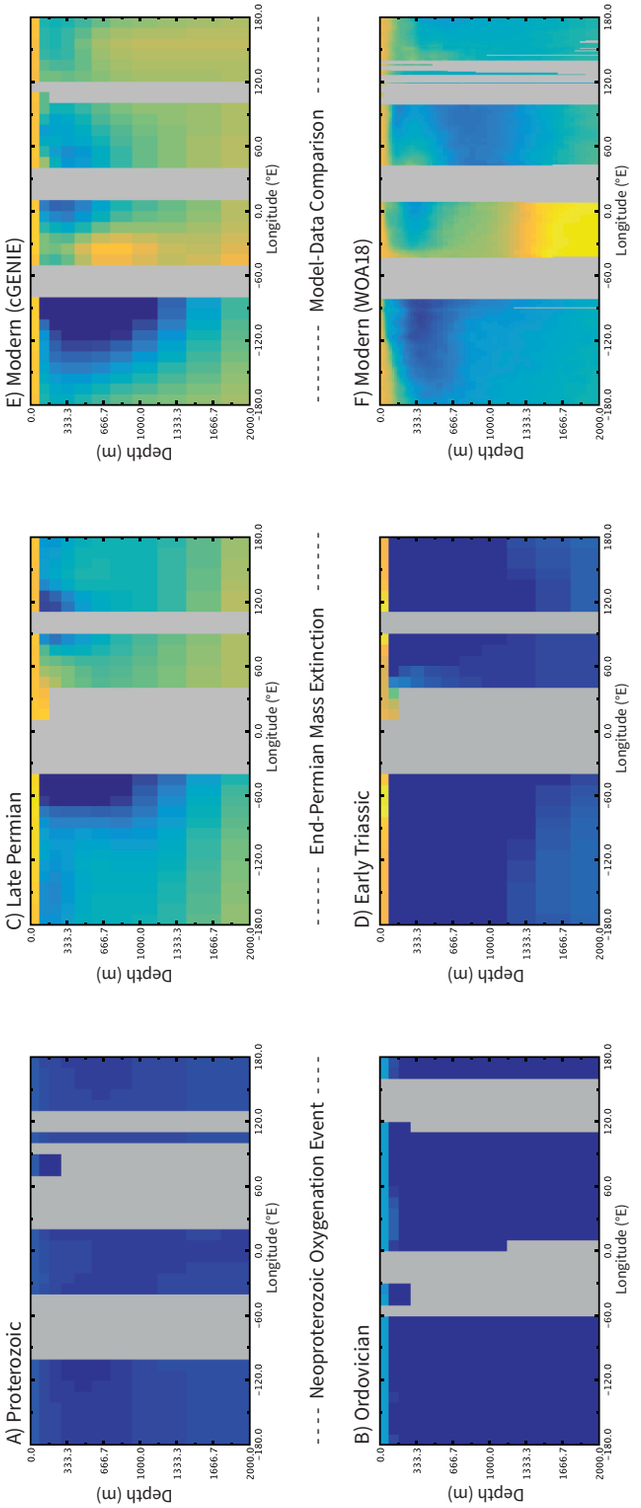

Figure 3. Equatorial transects of dissolved marine oxygen concentrations for a range of Earth system scenarios described in this review, comparing previously published ocean simulations generated using the cGENIE Earth system model (Ridgwell *et al.*, 2007) (A–E) to measured modern dissolved O_2 from the World Ocean Atlas (F). (A) Simulated Proterozoic dissolved O_2 profile, using a Cryogenian-Ediacaran continental configuration, 10% present atmospheric level (PAL) atmospheric O_2, and 0.05× modern marine PO_4 (Reinhard *et al.*, 2020). (B) Simulated early Paleozoic dissolved O_2 profile, using an Ordovician continental configuration, 40% PAL atmospheric O_2, and 1× modern marine PO_4 (Stockey *et al.*, 2021). (C) Simulated late Permian dissolved O_2 profile, reconstructing the background state preceding the end-Permian mass extinction, using a Permian continental configuration, 100% PAL atmospheric O_2, 1× modern marine PO_4, and 700 ppm CO_2 (Hülse *et al.*, 2021). (D) Simulated Early Triassic dissolved O_2 profile, reconstructing the main extinction phase of the end-Permian mass extinction, using a Permian continental configuration, 100% PAL atmospheric O_2, 2× modern marine PO_4, and 5600 ppm CO_2 (Hülse *et al.*, 2021). (E) Simulated modern dissolved O_2 profile, including temperature-dependent remineralization (Boscolo-Galazzo *et al.*, 2021). (F) Measured modern dissolved O_2 profile (Garcia *et al.*, 2019). All near-equatorial latitudinal transects are plotted as annual means at about 1.5°S, following the cGENIE grid structure and with vertical gray bars representing continents.

these approximate levels since this time (Scott and Glasspool, 2006). Thus, from the middle Paleozoic onward, surface oceans would have been in equilibrium with an atmosphere with near-modern oxygen. The deep ocean would have been fully ventilated (*i.e.*, Fig. 3C), excepting any vagaries of polar deep-water formation as related to plate tectonics and climate, which do not show any directional trends over this time. Any changes in the strength of the biological pump through time could also have impacted the distribution of oxygen in the ocean's interior (Meyer *et al.*, 2016), but the degree to which such changes occurred is debated (Fakhraee *et al.*, 2020). Importantly, for the past 420 million years, anoxic or dysoxic settings in the oceans would have had the same general oceanographic drivers as in the modern ocean (Fig. 3C, F). Specifically, deoxygenation would have developed beneath areas of higher primary productivity (in oxygen minimum zones [OMZs] and during times with higher nutrient inputs to the oceans) in enclosed seaways with limited deep-water renewal and, more broadly, in the open ocean because of stratification (Breitburg *et al.*, 2018; Levin, 2018).

Between the initial onset of oxygen in Earth's atmosphere at the GOE (~2200 million years ago) and the unquestioned onset of near-modern atmospheric oxygen levels (~420 million years ago), the situation is murkier. Here, geochemists must use observations of marine redox conditions and try to back-calculate atmospheric oxygen. Oxygen levels during the mid-Proterozoic, or Earth's Middle Age, between ~1800 and 800 million years ago, have generally been hypothesized to be between 1% and 10% PAL (Kump, 2008; Lyons *et al.*, 2014). However, this oxygen estimate represents to some extent the gut feeling of Earth historians. This is derived from observations that many shallow mid-Proterozoic waters remained oxic (*e.g.*, Shen *et al.*, 2003; Hardisty *et al.*, 2014) and from modeling results demonstrating that the invariably anoxic conditions in the deeper oceans would not have been present at higher than ~40% PAL (Canfield, 1998; Ozaki and Tajika, 2013; Cole *et al.*, 2022). The tricky question remains, though: exactly how low was atmospheric oxygen in Earth's Middle Age? Certainly, recent papers with large numbers of geochemical observations from I/Ca (Lu *et al.*, 2018), uranium isotopes (Gilleaudeau *et al.*, 2019), and iron speciation (Planavsky *et al.*, 2011; Sperling *et al.*, 2015b) have supported the view of a very weakly oxygenated mid-Proterozoic Earth system. But converting such observations into hard numbers is difficult. For instance, Bellefroid *et al.* (2018) modeled cerium anomaly data to indicate a vanishingly low <0.1% PAL O_2, whereas modeling of similar data by Liu *et al.* (2021) resulted in estimates of 1%–2% PAL. While both of these estimates unambiguously point to lower levels than likely existed in the later Neoproterozoic or Paleozoic, as discussed below (see *Oxygen and the origin of animals*), this order-of-magnitude difference has important implications for the role of oxygen in the origin of animals. Thus, the current aim is distinguishing whether mid-Proterozoic oxygen levels were simply low or rather exceedingly low. There has also been increasing emphasis on treating this billion years of Earth history with more temporal nuance (Canfield, 2014; Diamond and Lyons, 2018; Planavsky *et al.*, 2018).

The second canonical step in Earth's oxygenation history was generally believed to have occurred in the late Neoproterozoic, but whether this resulted in full oxygenation of the ocean-atmosphere system to modern levels has recently been thrown into question. Although there is clear geochemical proxy evidence for oxygenation in the Neoproterozoic, there is also proxy evidence for deoxygenation, and much of the prior evidence for a state change at this time is less clear (discussed by Cole *et al.*, 2020). Most likely, oxygen levels did rise around the base of the Cambrian, and the oceans were perhaps temporarily well oxygenated with respect to the remainder of the early Paleozoic (*e.g.*, Chen *et al.*, 2015; Wei *et al.*, 2018). However, persistent and widespread anoxic conditions in the deeper waters of early Paleozoic oceans (Berry and Wilde, 1978; Lu *et al.*, 2018; Dahl *et al.*, 2019; Gill *et al.*, 2021; Sperling *et al.*, 2021) suggest that the broad constraint provided by modeling for atmospheric O_2 (*e.g.*, <40% PAL) continues to apply to this interval. This inference is consistent with the latest generations of carbon cycle models (Krause *et al.*, 2018; Lenton *et al.*, 2018). The presence of Cambrian animals themselves does provide a new minimum estimate for Paleozoic oxygen levels, which was estimated by Sperling *et al.* (2015b) as ~10% PAL. While this does provide an increase in minimum oxygen levels (Fig. 1), because late Neoproterozoic levels are only loosely constrained, the magnitude of any late Neoproterozoic-early Cambrian oxygen increase (and whether it represented a step change) is unclear. Full oxygenation of the ocean-atmosphere system to 100% PAL likely occurred later in the Paleozoic (Dahl *et al.*, 2010; Wallace *et al.*, 2017; reviewed by Reinhard and Planavsky, 2022). Current research is focused on the magnitude of Paleozoic oxygenation (and deoxygenation) events and possible links between plant evolution and later Paleozoic oxygenation (Dahl and Arens, 2020).

Large Igneous Provinces and Their Effects

After the atmosphere reached 100% PAL, most deoxygenation events developed as a result of massive inputs of carbon to the Earth system as supplied by LIP eruptions. The LIPs and their extrusive flood basalts are voluminous outpourings of basaltic magma that occur over a relatively short time period (geologically speaking, <5 million years [Myr] and generally <1 Myr) (Kasbohm *et al.*, 2021). They occur in the middle of both oceanic and continental tectonic plates and are likely sourced from mantle plumes (making them fundamentally different in style of volcanism and size from any volcanic process currently operating on Earth). The flood basalt deposits from LIPs are often called trap rocks (the Siberian Traps, Deccan Traps, *etc.*) after the Swedish word *trappa* ("staircase"). This is due to the characteristic

stairstep morphology of the successive basaltic lava flows (Fig. 4B). In addition to the aboveground flood basalts, LIPs have a complex underground plumbing system of dikes and sills that can often intrude into and volatilize organic- or sulfur-rich sedimentary rocks, thereby dramatically increasing the CO_2 or sulfur aerosols that are emitted to the atmosphere (Ganino and Arndt, 2009; Svensen *et al.*, 2009).

High-precision geochronology has demonstrated that LIPs are precisely associated with multiple mass extinctions, including the three most recent Big Five extinctions (the five largest mass extinctions of the past 540 million years). The LIPs with precise links to extinctions include the second pulse of the North Atlantic Igneous Province (LIP)/Paleocene-Eocene Thermal Maximum extinction (PETM) (55.8 Ma), the Decan Traps/Cretaceous-Paleogene extinction (66.0 Ma), the Karoo-Ferrar/Pliensbachian-Toarcian boundary (182.7 Ma), the Central Atlantic Magmatic Province/Triassic-Jurassic boundary (201.5 Ma), and the Siberian Traps/Permian-Triassic boundary (251.9 Ma) (Ernst *et al.*, 2020; Kasbohm *et al.*, 2021). In these best-dated instances, the LIP erupted several hundred thousand years prior to the extinction (though note that both LIPs and extinctions may have multiple pulses). There are also LIPs likely associated with the Cretaceous ocean anoxic events at the Cenomanian-Turonian boundary (OAE-2) (93.9 Ma) and in the early Aptian (OAE-1a) (~121 Ma), the end-Guadalupian extinction (259.1 Ma), the Frasnian-Fammenian mass extinction (372.2 Ma), and the early-middle Cambrian extinction (~509 Ma), although the radiometric constraints are not as precise (Ernst *et al.*, 2020; Kasbohm *et al.*, 2021). Still other mass extinctions may be associated with LIPs, but this is based on indirect geochemical proxy evidence rather than a directly dated LIP (*e.g.*, for

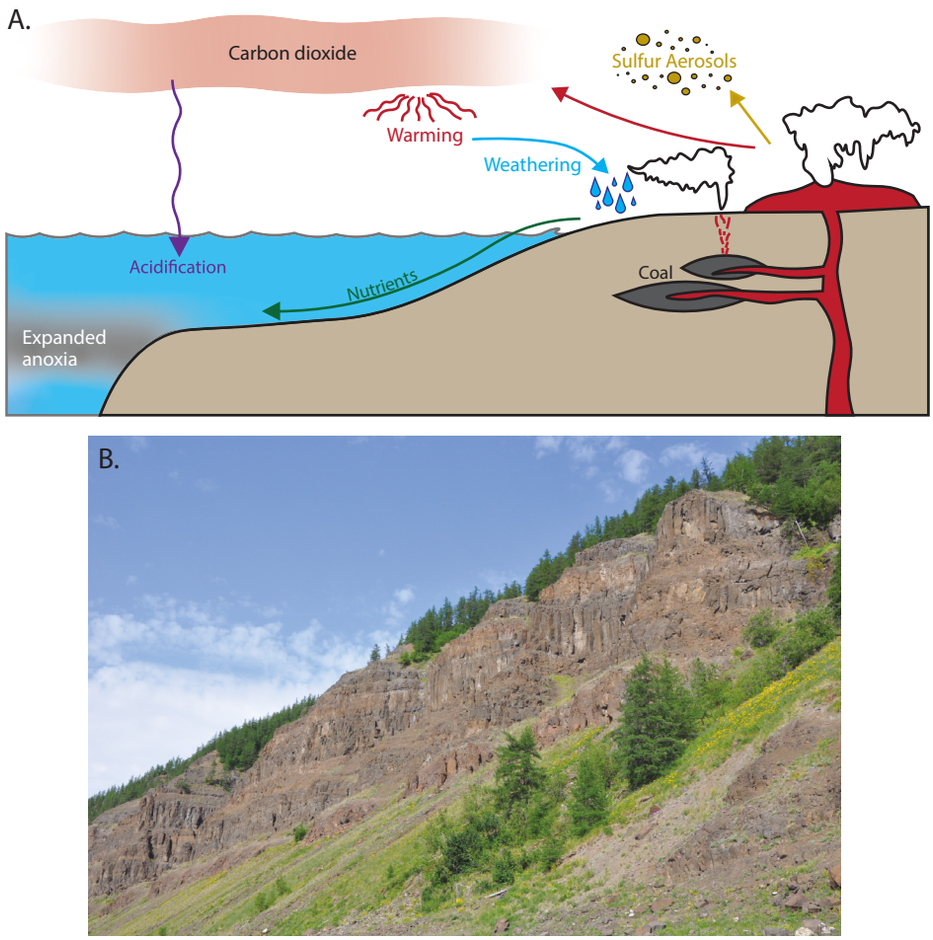

Figure 4. (A) Large igneous provinces (LIPs) are massive volcanic eruptions and the likely ultimate cause of most Phanerozoic mass extinctions. The eruption of CO_2 from these volcanic provinces (plus volatilized material they intrude into, such as organic rich shale and coal) results in global warming, ocean acidification, and ocean deoxygenation. Expanded ocean anoxia likely results from a combination of stratification, temperature-dependent remineralization, and increased terrestrial nutrient inputs from increased weathering on a warmer, wetter Earth. The exact oceanographic causes of anoxia are an area of active research. Modified from Clapham and Renne (2019). Used with permission of *Annual Reviews*. (B) Flood basalts of the Siberian Traps on the Kotuy River, Arctic Siberia. The lavas from this eruption cover a minimum area of ~3.5 million square kilometers, a land area larger than India and just smaller than the entire European Union. This eruption is responsible for the end-Permian mass extinction *via* deoxygenation and warming. Photo credit: Ben Black (Rutgers University).

the Late Ordovician extinction, Jones *et al.*, 2017; Hu *et al.*, 2020). Known LIP-extinction couplets are associated with geochemical evidence for both warming and deoxygenation (Fig. 4A; Ernst and Youbi, 2017). Reviewing the geochemical evidence for deoxygenation associated with LIPs/mass extinctions is beyond the scope of this article, but to focus on our highlighted proxy of uranium isotopes, a negative $\delta^{238}U$ shift—indicating widespread marine anoxia—has been documented in association with the Frasnian-Fammenian extinction (Song *et al.*, 2017; White *et al.*, 2018), Permian-Triassic extinction (Brennecka *et al.*, 2011; Lau *et al.*, 2016; Zhang *et al.*, 2018), Triassic-Jurassic extinction (Jost *et al.*, 2017), Cenomanian-Turonian boundary (Clarkson *et al.*, 2018), and PETM (Clarkson *et al.*, 2021). All other LIP-associated extinctions show evidence for widespread anoxia *via* other proxy methods (*e.g.*, thallium isotopes at the Pliensbachian-Toarcian boundary) (Them *et al.*, 2018). Current research focuses on understanding the nexus of eruption magnitude, rate, and aerosol release, combined with Earth system boundary state, that causes some LIPs to be deadlier than others (*e.g.*, Fig. 5B).

The Fossil Record

To understand the role of oxygen in animal evolution and biodiversity dynamics, it is necessary to understand how paleontologists read the fossil record and the nature of that record. For almost the entirety of Earth history (~85%), the fossil record was dominated by microbes, and even those fossils were relatively rare. Consequently, quantitative studies of Precambrian diversity have been difficult (discussed by Cohen and Macdonald, 2015). However, increased scrutiny of older rocks has revealed that the first total-group eukaryotes appeared around 1650 Ma (represented by larger cells with cell wall protrusions and possible nuclei) and the first unambiguous crown-group eukaryotes (the red algae *Bangiomorpha*) around 1050 Ma (reviewed by Agić, 2021). Molecular clocks suggest that the animal crown group originated around 800 Ma (Dohrmann and Wörheide, 2017), although undoubted animal fossils are not present until the end of the Neoproterozoic, in the so-called Ediacaran fauna. The ~50 million years spanning the Precambrian-Phanerozoic boundary witnessed the appearance of essentially all fossilizable animal phyla and classes (Erwin *et al.*, 2011; the Cambrian explosion; Fig. 1). The explosive aspect of this event is with respect to the appearance of high-level animal body plans (disparity) rather than species diversity and with respect to the three billion years of preceding geological record with no animal fossils. Focusing on the ~50 million years from 570 to 520 Ma, however, it rather reflects a protracted series of evolutionary innovations and radiations (Wood *et al.*, 2019).

Following the Cambrian radiation, paleontologists have been able to better tabulate and statistically analyze the diversity of life on Earth. The most recognizable and influential Phanerozoic diversity curve of fossil animals is the Sepkoski curve (Sepkoski, 1981). This curve is based on a compendium that consists of first and last known fossil occurrences with a temporal resolution down to the geologic stage (the smallest geologic time subdivision) of marine

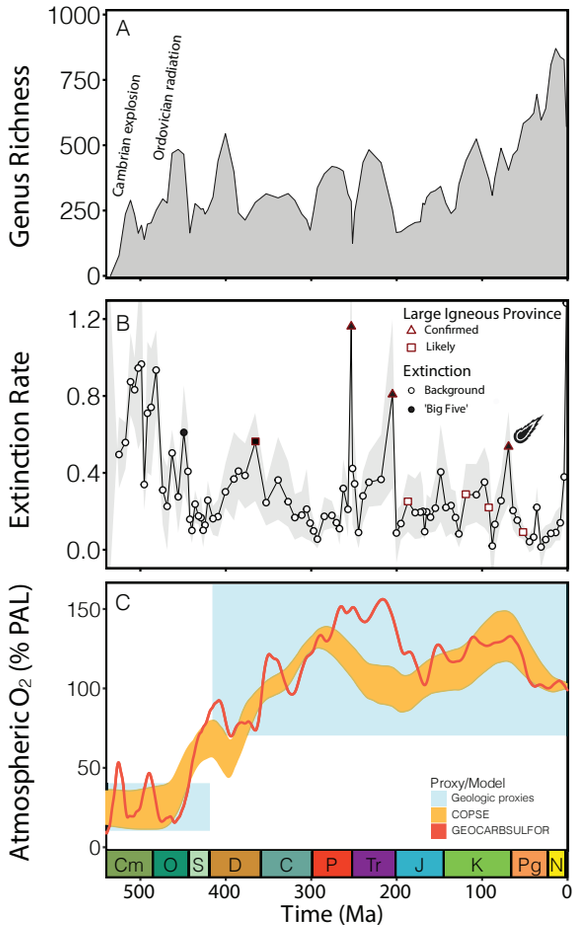

Figure 5. Reconstructed marine animal biodiversity dynamics and atmospheric oxygen through the Phanerozoic (comprising the Paleozoic, Mesozoic, and Cenozoic eras; the past 540 million years of Earth history). (A) Genus diversity for marine animals at stage-level resolution, reconstructed using shareholder quorum subsampling (replotted from Kocsis *et al.*, 2019). (B) Genus extinction rates for marine animals at stage-level resolution, replotted from Kocsis *et al.* (2019) following Stockey *et al.* (2021). Line and points represent means of 12 extinction rate metrics for each stage, while envelopes represent minimum and maximum values. Following paleontological convention, the points are plotted as mid-points of geological stages and so will not directly correspond to precise geochronological constraints for large igneous provinces (LIPs). Relationship between LIPs and extinctions follows Ernst *et al.* (2020) and Kasbohm *et al.* (2021). The Cretaceous-Paleogene mass extinction at 66 Ma was primarily caused by a meteorite impact. (C) Reconstructed atmospheric O_2 expressed as a percentage of present atmospheric levels (% PAL), but on linear rather than log scale. Shown are long-term carbon cycle model estimates (Krause *et al.*, 2018; Lenton *et al.*, 2018) and geological or geochemical proxies. Adapted from Stockey *et al.* (2021). Abbreviations for geologic time periods: Cm, Cambrian; O, Ordovician; S, Silurian; D, Devonian; C, Carboniferous; P, Permian; Tr, Triassic; J, Jurassic; K, Cretaceous; Pg, Paleogene; N, Neogene.

animal orders, families, and genera from the published literature. Sepkoski demonstrated that there has been an increase in diversity across the Phanerozoic that follows a logistic curve (Fig. 5A). The general shape of the curve starts with a sharp increase during the Cambrian (Cambrian explosion), followed by a short plateau that is then followed by a larger increase during the Ordovician (Great Ordovician Biodiversification Event) before plateauing during much of the Paleozoic. This plateau is ultimately followed by an unabated increase to the Modern, starting during the early Mesozoic (Sepkoski, 1981). Recently, the compilation of fossil occurrences in the Paleobiology Database (2022) has enabled quantitative paleobiologists to address sampling biases in reconstructions of biodiversity, extinction, and origination through the Phanerozoic (Fig. 5; Alroy *et al.*, 2008; Alroy, 2010; Kocsis *et al.*, 2019).

Perhaps the most influential outcome of Sepkoski's compendium is the first quantitative recognition of major mass extinction events. Extinctions in the fossil record were previously known, but Sepkoski's compendium made it possible to estimate the magnitude and temporal resolution of these events (Raup and Sepkoski, 1982). Raup and Sepkoski (1982) revealed the occurrence of five major mass extinction events (colloquially named the Big Five) as having occurred during the Late Ordovician (~445 Ma), Late Devonian (~370 Ma), end-Permian (~252 Ma), end-Triassic (~201 Ma), and end-Cretaceous (~66 Ma). The recognition of these extinction events spurred a flurry of new research agendas dedicated to uncovering the causal mechanisms. While there are open questions associated with all mass extinction events, the general consensus is that, for extinctions after atmospheric oxygen levels reached ~100% PAL, the most common ultimate cause is the activity of LIPs, and the most likely proximate cause is the downstream environmental impacts including warming and deoxygenation (Bond and Grasby, 2017; Clapham and Renne, 2019; Fig. 4). The primary exception is the end-Cretaceous extinction event, which is primarily attributed to a bolide impact (Alvarez *et al.*, 1980; Hull *et al.*, 2020), although the temporal coincidence with the Deccan Traps LIP complicates causal scenarios (Schoene *et al.*, 2015).

In addition to identifying five major mass extinction events, Raup and Sepkoski (1982) also noted that background extinction has gradually decreased across the Phanerozoic. Specifically, the total extinction rate (family extinctions per million years) was greatest during the Cambrian but gradually decreased over the next 500 million years. Subsequent studies that better account for possible sampling biases have also observed this decrease in extinction rate (*e.g.*, Foote, 2003; Alroy, 2008; Kocsis *et al.*, 2019). Various causal mechanisms have been proposed to explain the decrease in extinction rates, including increased ecological complexity, ecological resistance to extinction, taxonomic structure (increase in the number of species per clade over time), lineage durations, variability of the rock record, and stabilization of the carbon cycle as a result of decreased shallow-marine anoxia (reviewed by Payne *et al.*, 2020). These observations remain largely correlative, and no community-wide consensus has yet been established.

Connecting Geochemistry and Fossils through Physiology

Traditionally, geochemical data have been compared stratigraphically with paleontological diversity data to assess the environmental impact of a given oxygenation or deoxygenation event. Here, we attempt to interpret these coupled records in light of information from modern physiology and ecology (Knoll, 2013). In particular, our interpretation of possible links between oxygen and the development of animal multicellularity are based on observations from respiration experiments on body plan analogs of the earliest animals, whereas our interpretation of the Cambrian radiation is based on space-for-time substitutions (*e.g.*, Blois *et al.*, 2013) from modern OMZs. Moving into the Phanerozoic, we focus on the metabolic index (Deutsch *et al.*, 2015) as an ecophysiological link between environment and organismal evolution. The metabolic index (Φ) incorporates both environmental parameters (the partial pressure of oxygen [pO_2] and temperature [T]) and species-specific physiological parameters (A_o, E_o, and n) to predict the balance between organismal oxygen supply and demand (Equation 1), which must be greater than 1 for habitat to be aerobically viable. The parameter A_o represents an organism's hypoxia tolerance (at a reference temperature in some formulations), E_o represents how hypoxia tolerance changes with temperature, and n represents the allometric scaling of an organism's oxygen supply and demand balance with its body size (B). These physiological parameters are calibrated using respirometry experiments in which the lowest pO_2 that can sustain an organism's standard metabolic rate, or P_{crit}, is measured across a range of temperatures. Note that a number of minor variations of the metabolic index equation have been applied to different ecophysiological problems since its development by Deutsch *et al.* (2015), but all are solving the same problem of viable aerobic habitat:

$$\Phi = A_o \cdot B^n \frac{pO_2}{\exp\left(\frac{-E_o}{k_B \cdot T}\right)}. \quad (1)$$

Simply put, Φ is the ratio of environmental oxygen supply to metabolic oxygen demand of a species, given the combination of local temperature and oxygen conditions. At $\Phi = 1$, there is exactly enough oxygen in a given area for the species to maintain standard metabolic rate (SMR). At $\Phi > 1$, the species has that many more times the environmental oxygen available to it than it needs to maintain SMR. Conversely, at $\Phi < 1$, the species does not have enough environmental oxygen supply to meet its standard metabolic oxygen demand; thus, that given area would be aerobically unsustainable. Marine organisms do not, however, occupy

all areas of the ocean where $\Phi > 1$; this is because organisms are performing physiological functions, such as growth, reproduction, or feeding, that require a greater amount of oxygen than what is needed to maintain SMR. The term Φ_{crit} is the lowest Φ value where a given species is documented to exist and is considered the minimum Φ value required for the persistence of that species in a particular area (Deutsch *et al.*, 2015, 2020).

Oxygen and Animals in the Precambrian and Paleozoic

Oxygen and the origin of animals

In 1959, the biologist John Nursall argued that the lack of Proterozoic animal fossils was a real reflection of the absence of animal life. Citing Harold Urey (1952), who argued that the atmosphere must have remained reducing until at least 800 Ma, Nursall (1959) suggested that the permanent oxygenation of the atmosphere occurred between 800 and 600 Ma, immediately preceding the origin of aerobic life and the explosive (tachytelic) diversification of animals across the Precambrian-Cambrian boundary. While the permanent oxygenation of the atmosphere (the GOE) is now constrained to ~2.22 billion years ago (Ga) (Poulton *et al.*, 2021), the idea that atmospheric oxygen remained too low to support multicellular animals (*e.g.*, Cloud, 1976), or at least fossilizable animals (*e.g.*, Towe, 1970; Runnegar, 1982a), until the late Proterozoic nevertheless stuck—primarily among geochemists reconstructing ancient oxygen levels (reviewed by Mills and Canfield, 2014). The exact physiological mechanisms underlying this prediction, however, either remained vague or varied from model to model. For the origin of animals from unicellular protists, one proposed mechanism concerned the amount of ambient oxygen needed to meet the oxygen demands of the earliest diffusion-dependent animals (Cloud, 1976). For the origin of animals capable of entering the fossil record, one mechanism concerned the amount of oxygen needed to surpass the basic oxygen requirement for collagen synthesis and to permit the secretion of shells, cuticles, and other "hard parts" (Towe, 1970). Many of these earlier proposed mechanisms, such as the oxygen requirement for collagen, have since been refuted (reviewed by Cole *et al.*, 2020) and none have arisen in their stead.

Given current data, it is unlikely that oxygen was limiting for multicellular animals unless it was far below the generally hypothesized mid-Proterozoic level of 1%–10% PAL. Most pertinent to this discussion, the earliest animals were likely soft-bodied diploblasts (animals possessing only two germ layers, an inner and an outer), an organization that essentially leaves all respiring cells in diffusive contact with seawater (Runnegar, 1982b; Sperling *et al.*, 2013b). Thus, the minimal oxygen requirements for the earliest animals were unlikely to have been considerably different from those of unicellular eukaryotes, which had existed for hundreds of millions of years before (Fig. 1). Concordant with this interpretation, respirometry data indicate that modern marine sponges (diploblastic and perhaps similar in body plan to some of the earliest animals) can survive under the oxygen levels estimated to have characterized the mid-Proterozoic surface oceans (Mills *et al.*, 2014, 2018; Micaroni *et al.*, 2021). Animals additionally conserve a limited subset of genes for enzymes catalyzing anaerobic energy metabolism pathways, which are distributed widely throughout the metazoan tree, enabling animals to spend extended portions of their life cycles under anoxia (Müller *et al.*, 2012; Mentel *et al.*, 2014). These physiological and genomic observations, as well as the fact that animals are monophyletic (an evolutionary novelty), suggest that the attainment of environmental oxygen levels permissive to animals—while a prerequisite—was not the primary control on when animal life originated in geologic time (*e.g.*, Butterfield, 2009b). The evolution of multicellularity in animals and other Neoproterozoic eukaryotes was more likely related to food supply or feeding rather than oxygen (Leys and Kahn, 2018; Butterfield, 2020). The caveat to this would be if mid-Proterozoic and early Neoproterozoic oxygen levels were exceptionally low (*i.e.*, <0.1% PAL, which we view as unlikely but possible). Specifically, the order of magnitude difference between 0.1% and 1.0% PAL is key. If oxygen levels prior to ~800 Ma were persistently <0.1% PAL, then the marine environment was likely not permissive to animals; levels between 0.1% and 1.0% are ambiguous and require consideration of the temporal persistence of anoxic events and synergistic factors, such as temperature (Reinhard *et al.*, 2016); and persistent levels >1.0% suggest sufficient oxygen for early animals well prior to their appearance.

Oxygen and the early radiation(s) of animals

While the earliest animals and earliest bilaterians may not have been limited by low Proterozoic oxygen levels, oxygen availability may have been limiting for the evolution of larger, armored (biomineralized), and more active animal body plans that developed across the Precambrian-Cambrian boundary independently in several clades. In contrast to the monophyletic origin of animals, this polyphyletic radiation in the Cambrian suggests an extrinsic (environmental) control. In a classic paper, Rhoads and Morse (1971) reviewed the biological oceanography of modern OMZs and demonstrated that changes in body size, diversity, and bioturbation with increasing oxygen broadly re-capitulated the appearance of animals across the Precambrian-Cambrian boundary. This space-for-time substitution was a key observation linking Cambrian oxygenation with the biological radiation, and their insights have been supported by four further decades of study in OMZs. New observations have added two nuances to the story. First, Sperling *et al.* (2013a) studied how polychaete feeding ecology changed across oxygen gradients in modern OMZs and demonstrated that while polychaetes can live at very low (~suboxic) oxygen levels, carnivorous polychaetes generally do not. The

study found a clear relationship between increasing oxygen levels and the abundance and diversity of carnivores, which is not unexpected, given the O_2 requirements for mobility and digestion in this feeding strategy. The recent demonstration that vision in marine invertebrates is highly oxygen dependent (McCormick *et al.*, 2019) further links oxygen and carnivory, given the importance of visual acuity in predation (Parker, 2003). The advent of carnivory and resulting predator-prey arms races represents the most plausible causal factor in the appearance of new animal body plans (which is what characterizes the Cambrian radiation) (Peterson *et al.*, 2005; Marshall, 2006; Dzik, 2007; Butterfield, 2009a); given this, we can draw a causal scenario linking oxygen, ecology, and macroevolution. Specifically, we can hypothesize that the earliest animals were limited to small body sizes and low-energy feeding strategies and that an increase in oxygen levels allowed for more active, carnivorous feeding strategies that ultimately ignited the Cambrian explosion.

The second recent observation is that, compared to Rhoads and Morse (1971), we know that the critical oxygen thresholds that would permit Cambrian-type animals *versus* prohibit them are quite low (Sperling *et al.*, 2015a). As noted above, based on ecological patterns in modern OMZs, ~10% PAL would likely be sufficient. Based on the known oxygen constraints (Fig. 1), changes in oxygen are a plausible trigger for the Cambrian explosion, but equally plausible is that oxygen increased substantially around the base of the Cambrian but is only coincidentally correlated with the biological radiation. As an example, an increase from a Neoproterozoic baseline of 15% to 30% PAL in the Cambrian represents a doubling of atmospheric oxygen; but such an oxygen increase would have likely played a relatively minor role in animal evolution, because there was sufficient oxygen for Cambrian-type organisms (including predators) prior to that time. Alternatively, a doubling from a Neoproterozoic baseline of 5% to 10% in the Cambrian would cross the critical ecological thresholds and allow the causal scenario described above to hold. Thus, despite much progress in both geochemistry and paleobiology, increased resolution of the actual magnitude of oxygenation and the oxygen requirements of the Cambrian fauna are still required to satisfactorily understand the role of oxygen in the Cambrian explosion. Changes in oxygen or marine redox have also been invoked to explain the major increase in lower taxonomic diversity during the Ordovician radiation (Fig. 5A; Saltzman *et al.*, 2015; Marenco *et al.*, 2016; Edwards *et al.*, 2017). While this role for oxygen remains a possibility, like the hypotheses relating oxygen and the origin of animal multicellularity, the evolutionary or ecological mechanisms by which increasing oxygen facilitated this radiation are not clear or differ between studies. In addition to more focus on evolutionary mechanisms for both radiations, researchers must better incorporate other environmental factors such as food supply or productivity (Pohl *et al.*, 2018; Sperling and Stockey, 2018) and temperature (Boag *et al.*, 2018; Goldberg *et al.*, 2021); oxygen is a critical environmental variable but far from the only one.

Oxygen and early Paleozoic extinctions

Although the dawn of the Paleozoic witnessed these two major evolutionary radiations, the early Paleozoic was also characterized by anomalously high extinction rates relative to the remainder of the Phanerozoic. A new ecophysiological explanation for high early Paleozoic extinction rates was recently proposed that requires only commonplace climatic perturbations in the context of lower atmospheric oxygen levels (Stockey *et al.*, 2021; Figs. 5, 6). Our understanding of the synergistic effects of oxygen and temperature predicts that marine ectotherms are likely to have smaller thermal safety margins at lower environmental oxygen levels (Pörtner, 2010; Deutsch *et al.*, 2015). Marine animals are therefore expected to be more vulnerable during ocean warming events in low-oxygen Earth system states. Stockey *et al.* (2021) generated 3D ocean simulations using the cGENIE Earth system model (Ridgwell *et al.*, 2007) at different atmospheric O_2 levels, continental configurations, and climate states. These ocean models were then combined with the metabolic index framework (Deutsch *et al.*, 2015; Penn *et al.*, 2018; Equation 1) to estimate the magnitude of warming-driven extinction for a given climate perturbation under different levels of atmospheric oxygenation. Specifically, the modeled ancient oceans were populated with ecophysiotypes

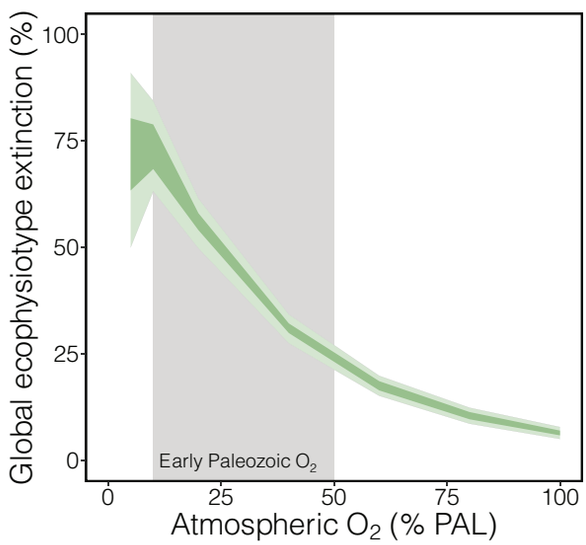

Figure 6. The metabolic index demonstrates that animals are likely to have less aerobic safety buffer with respect to warming events under lower atmospheric oxygen levels. Figure shows global ecophysiotype extinction predicted to result from a ~5 °C warming event from an approximately pre-industrial baseline sea surface temperature at different atmospheric O_2 levels. Darker envelopes represent 25th–75th percentiles of 100 simulation results; lighter envelopes represent 5th–95th percentiles. Modified from Stockey *et al.* (2021), which also includes additional sensitivity analyses. % PAL, percentage of present atmospheric levels.

having physiological parameters drawn from the distributions measured in modern species (namely, A_o, E_o, and Φ_{crit}). The ocean was then perturbed with a CO_2-driven warming event, and the percentage of ecophysiotypes that could find viable aerobic habitat before the warming event was compared to the post-warming ocean. The modeled marine extinction events resulting from standard climate variability under early Paleozoic levels of oxygenation were much more severe than those predicted for the same climate perturbation under modern atmospheric oxygen levels (Fig. 5). Notably, these analyses illustrate an inflection point in simulated extinction magnitude around the upper limit for reconstructed early Paleozoic oxygenation. This modeling approach further demonstrates that atmospheric oxygen is a more important factor in controlling the extinction vulnerability of marine ectotherms than other Earth system boundary conditions such as continental configuration, pre-warming climate state, and the strength of the biological pump.

Anatomy of a Mass Extinction: Permian-Triassic Mass Extinction

The end-Permian mass extinction was the most severe biotic crisis in the history of animal life, whether measured in terms of the proportion of taxa lost (Raup and Sepkoski, 1982; Benton, 1995) or the impact on ecosystem structure (Droser *et al.*, 2000). Many causes have been proposed for this global catastrophe (reviewed in Erwin, 1993; Payne and Clapham, 2012), but emerging data from sedimentary geology and geochemistry and new insights from animal physiology demonstrate that stresses impacting respiratory physiology can account for both taxonomic and biogeographic selectivity patterns in the extinction (Knoll *et al.*, 1996, 2007; Clapham and Payne, 2011; Kiessling and Simpson, 2011; Penn *et al.*, 2018; Song *et al.*, 2020; Foster *et al.*, 2022).

Most researchers now agree that the eruption of the Siberian Traps, the largest LIP of the past 500 million years, was the geological event that triggered the environmental changes responsible for the biodiversity crisis (*e.g.*, Renne and Basu, 1991; Campbell *et al.*, 1992; Reichow *et al.*, 2009; Svensen *et al.*, 2009; Burgess and Bowring, 2015; Burgess *et al.*, 2017; Fig. 7). The global environmental impact of the Siberian Traps eruptions resulted from the release of volcanic gases, dominated by carbon dioxide but also including sulfur volatiles and halocarbons (Svensen *et al.*, 2009; Sobolev *et al.*, 2011; Black *et al.*, 2012; Broadley *et al.*, 2018; Elkins-Tanton *et al.*, 2020). The eruptions of this specific LIP likely had an outsized environmental impact because the gas content of the large volume of basaltic magma was enhanced *via* heating and degassing of volatile-rich sedimentary rocks (*i.e.*, coal) in the Tunguskaya Basin (Ganino and Arndt, 2009; Svensen *et al.*, 2009; Ogden and Sleep, 2012; Elkins-Tanton *et al.*, 2020). The discovery of coal fly ash at the Permian-Triassic boundary in sites far distant from the Siberian Traps provides further direct evidence

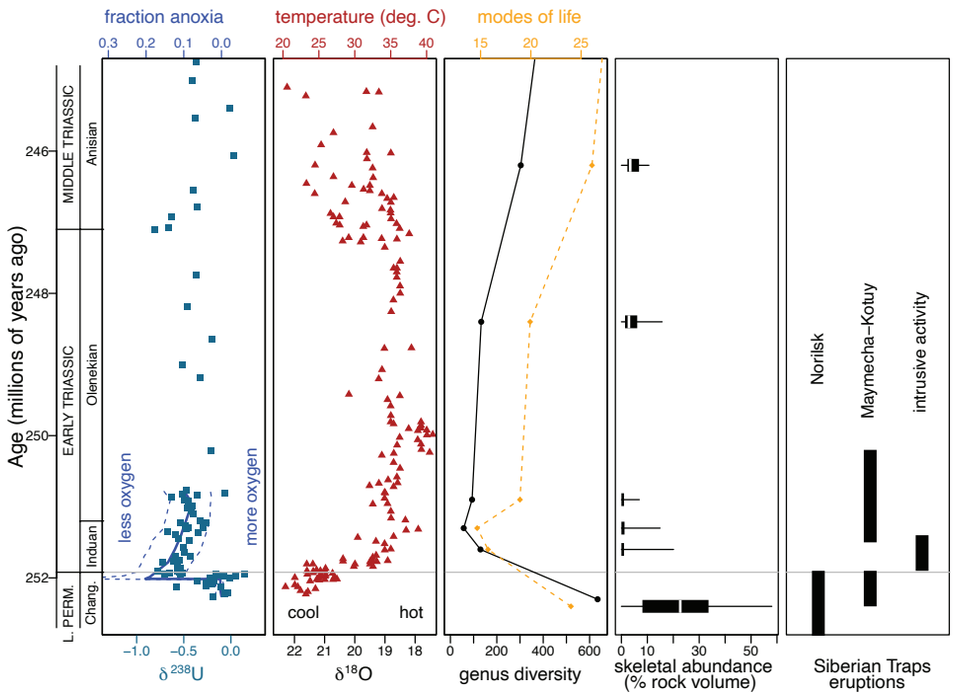

Figure 7. The chronology of the worst mass extinction in Earth history. From left to right, panels depict $\delta^{238}U$ (a proxy for the global redox landscape; isotope data from Lau *et al.*, 2016 and estimate of percentage of anoxic seafloor from Pimentel-Galvan *et al.*, 2022), $\delta^{18}O$ (a proxy for surface temperature; data from the Tethys ocean from Sun *et al.*, 2012), global genus diversity and ecological modes of life (replotted from Lau *et al.*, 2016), skeletal abundance in shallow marine sediments from South China (data from Payne *et al.*, 2006), and main eruptive episodes of the Siberian Traps large igneous province (data from Burgess and Bowring, 2015). Abbreviations for geologic time periods: Perm., Permian; Chang., Changhsingian.

for massive coal combustion and concomitant CO_2 release (Grasby *et al.*, 2011).

This massive injection of CO_2 into the Earth system caused substantial greenhouse warming and marine deoxygenation (Fig. 7). Seawater temperatures in the surface of the tropical Tethys Ocean increased ~12 °C within ~800 kyr, from ~25 °C to ~37 °C, with potentially 7 °C to 10 °C of warming occurring in ~39 kyr (Sun *et al.*, 2012). Accurate temperature estimates are unfortunately not available from most areas worldwide across the Permian-Triassic, although other temperature proxy records do concur there was substantial warming (*e.g.*, Joachimski *et al.*, 2012, 2019). It is essential to consider both magnitude and timescale of warming when comparing the end-Permian crisis with modern global change, because the late Permian warming was substantially larger but occurred over a much longer duration. With respect to deoxygenation, the series of oceanographic linkages between CO_2 injection and deoxygenation remain controversial. For instance, Penn *et al.* (2018), using the community earth system model (CESM), suggested that warming drove persistent stratification of the ocean and, thereby, anoxia, whereas Hülse *et al.* (2021), using the cGENIE Earth system model (Ridgwell *et al.*, 2007), suggested that widespread anoxia was largely the result of temperature-driven microbial respiration. Despite these uncertainties regarding the oceanographic mechanism of deoxygenation, it is now clear from geologic and geochemical evidence that ocean deoxygenation coincided with the end-Permian mass extinction and persisted for several million years into the Triassic.

Evidence of end-Permian ocean deoxygenation emerged first from analyses of sedimentation patterns, as many shallow-marine records exhibit shifts from light-colored, bioturbated sediments below the extinction horizon to dark-colored, unbioturbated sediments above the extinction horizon (Wignall and Hallam, 1992; Wignall and Twitchett, 1996). Similar sedimentological shifts occur in deep-marine stratigraphic sections as well (Isozaki, 1997). Iron speciation and pyrite framboid sizes demonstrate euxinic conditions developing in places at mid-shelf or even inner shelf depths during the end-Permian extinction, with ferruginous conditions present at deeper depths (Bond and Wignall, 2010; Clarkson *et al.*, 2016; Schobben *et al.*, 2020). Finally, in addition to these inorganic proxies, fossil molecules (biomarkers) derived from the pigments of green sulfur bacteria peak in abundance near the Permian-Triassic boundary (Grice *et al.*, 2005; Cao *et al.*, 2009). These bacteria photosynthesize using hydrogen sulfide as an electron donor, thus requiring anoxic, sulfide-bearing water within the marine photic zone. The occurrence of these fossil molecules at widely distributed sites indicates an unusual prevalence of shallow-marine euxinia associated with the mass extinction event.

Over the past decade, inferences from sedimentary patterns and local redox proxies have been strengthened *via* geochemical analysis of global redox proxies. Specifically, studies demonstrate that the Middle and Late Permian were characterized by $\delta^{238}U$ similar to the modern ocean, followed by a negative uranium isotope shift across the Permian-Triassic boundary in shallow-marine carbonate rocks. This uranium isotope excursion was first identified across the immediate Permian-Triassic boundary (Brennecka *et al.*, 2011), with later studies demonstrating that light $\delta^{238}U$ values characterized the entirety of the Lower Triassic and could be found in numerous locations worldwide, including south China, Iran, and Turkey (Lau *et al.*, 2016; Elrick *et al.*, 2017; Zhang *et al.*, 2018). Numerical models of the uranium cycle accounting for uncertainty in model parameters indicate that the shift in $\delta^{238}U$ requires a change in the areal extent of seafloor anoxia from <1% to >10% in less—and perhaps much less—than 50 kyr (Lau *et al.*, 2016; Kipp and Tissot, 2022; Pimentel-Galvan *et al.*, 2022; Fig. 7). Agreement between independent reconstructions of seafloor anoxia based on $\delta^{238}U$ and uranium concentration data further suggests that both datasets contain a strong original redox signature rather than local or diagenetic overprints (Pimentel-Galvan *et al.*, 2022).

It is now clear that the latest Permian ocean was similar to the modern in terms of both temperature and widespread oxygenation and that the mass extinction event occurred in association with a substantial increase in atmospheric carbon dioxide levels, climate warming, and ocean deoxygenation. The central challenge in using environmental paleoproxy data to infer extinction causes is the mapping between proxy data (environmental stress) and physiological response. The uranium isotope modeling indicates that anoxia was widespread (a best guess of 18% of the global seafloor in Pimentel-Galvan *et al.*, 2022). Anoxia was likely concentrated below storm wave base in outer shelf or slope environments, although truly anoxic and/or sulfidic conditions may have impinged into shallower water in some areas (Grice *et al.*, 2005; Schobben *et al.*, 2020). However, with near-modern atmospheric oxygen (*i.e.*, 100% PAL) it is nearly impossible to drive the entire ocean anoxic (Fig. 3E). This is particularly true for shallow waters in direct connection with the atmosphere, and indeed, well-aerated shoreface environments in the earliest Triassic can record robust and healthy animal communities (Beatty *et al.*, 2008). Given the difficulty of developing widespread anoxia in the locus of animal biodiversity (shallow shelf), most likely anoxia and/or euxinia was an important local or regional kill mechanism but not the global kill mechanism. Rather, geochemical evidence for increased anoxia in deeper-water settings (*e.g.*, light $\delta^{238}U$ carbonate values) are an indirect signal of the real killer: the development of widespread low-oxygen (dysoxic) conditions on the shelf combined with high temperatures.

Progress in understanding the relative biotic impact of these stressors has been made through a workflow incorporating (1) an Earth system model calibrated with available geochemical proxy data, (2) an ecophysiological model of temperature-dependent hypoxia (the metabolic index), and (3) comparison between model results and the fossil

record. Application of this approach to the end-Permian mass extinction demonstrates that changes in aerobic habitat due to ocean warming and resulting ocean deoxygenation can account for the observed latitudinal gradient and extinction intensity in the initial major pulse of end-Permian extinction (Penn *et al.*, 2018). Specifically, this study used a general circulation model with an end-Permian paleogeography to simulate a major climate warming event (*via* an increase in modeled partial pressure of carbon dioxide [pCO_2] from 150 to 5580 ppm). The resulting paleoceanographic model provided a good fit to available U isotope constraints and paleotemperature proxies (Sun *et al.*, 2012; Lau *et al.*, 2016). As discussed above with respect to early Paleozoic extinctions, the Penn *et al.* (2018) study also simulated "ecophysiotypes" by sampling from the distributions of physiological parameters measured in modern species. Similarly, the availability of aerobic habitat for these species within the model was assessed before and after the modeled CO_2 injection event.

The simulated pre-extinction ocean was habitable to at least some species in all regions, and aerobic habitat declined for nearly all species after the injection event as a result of the combined effects of deoxygenation and warming. Because of changes in the wind field, ocean currents, and primary productivity, the upper regions of the tropical ocean experienced substantial warming but little deoxygenation, whereas the polar regions experienced more substantial deoxygenation. Consequently, loss of aerobic habitat in the model was governed more by deoxygenation near the poles and more by warming near the equator (Fig. 8B). Overall, predicted loss of habitat and extinction was greater near the poles and lesser, albeit still substantial, in the tropics (Fig. 8B). Intriguingly, the ecophysiological model results also suggest that the latitudinal pattern of extinction intensity was driven as much by the spatial distribution of species with different physiological capacities in the pre-extinction Permian ocean as by the spatial pattern of environmental change during the event itself. Ecophysiotypes living in the tropics prior to the extinction were characterized by traits pre-adapted to warm, low-oxygen environments (low hypoxic thresholds and low ratios of active to resting metabolism, or Φ_{crit}) and were able to exploit such conditions when they arose globally. Conversely, higher latitudes in the pre-extinction ocean could support ecophysiotypes with high hypoxic thresholds and higher Φ_{crit}. These ecophysiotypes had no escape and were preferentially exterminated when the high latitudes warmed and lost oxygen.

Model predictions for the biogeography of the end-Permian mass extinction based on application of the metabolic index generally agree with evidence from the fossil record. Extinction was severe everywhere but eliminated a greater proportion of marine animal genera at temperate and high latitudes than in the tropics (Fig. 8A; Penn *et al.*, 2018). This latitude gradient in extinction does not appear

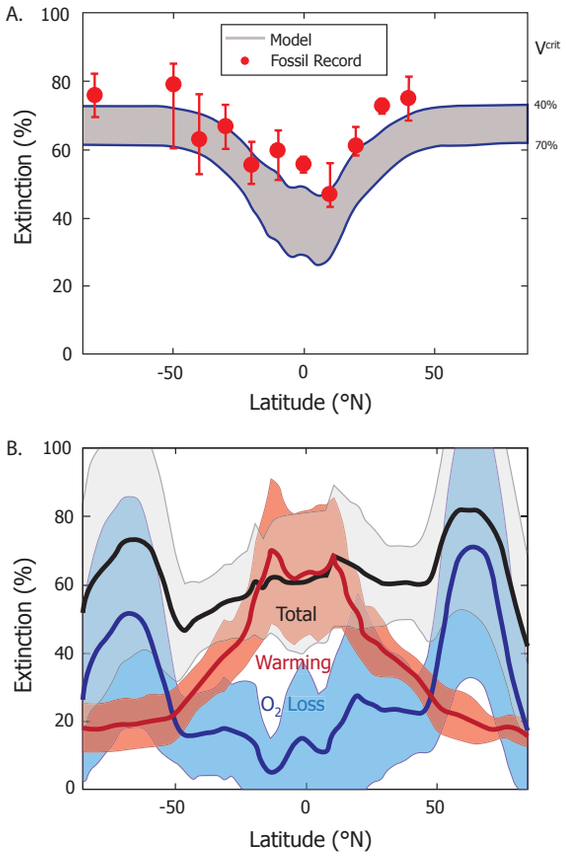

Figure 8. Ecophysiological modeling of the Permian-Triassic mass extinction. (A) Global extinction *versus* latitude, as observed in marine genera from end-Permian fossil occurrences in the Paleobiology Database (2022) and shown by red circles with error bars. Modeled extinction with the metabolic index based on simulated warming and deoxygenation is shown by the gray band. This analysis assumes a maximum possible depth of initial habitat of 500 m (suitable for the end-Permian fossil record) and varies between a fractional loss of 40% and 70% of habitat volume (V^{crit}) required to result in extinction. Both the fossil record and the ecophysiological model suggest higher extinction in polar regions compared to the tropics. Additional paleontological and modeling sensitivity analyses are shown in Penn *et al.* (2018). (B) Regional extinction (*i.e.*, extirpation) *versus* latitude for model ecophysiotypes across the Permian-Triassic extinction, with individual contributions from warming and the loss of seawater O_2 concentration. Extirpation occurs in locations where the metabolic index meets the active demand of an ecophysiotype in the Permian ($\Phi > \Phi_{crit}$) but falls below this threshold in the Triassic ($\Phi < \Phi_{crit}$).

to reflect variation in the quality of the fossil record before and after the extinction and appears independently in analyses separating the phyla with more sophisticated respiratory and circulatory systems and greater motility (Arthropoda, Chordata, Mollusca) from other well-fossilized phyla (Bryozoa, Brachiopoda, Cnidaria, Echinodermata) (Penn *et al.*, 2018, fig. S14A). The model thus does not currently explain the difference in extinction intensity across classes and phyla identified by Knoll *et al.* (1996), suggesting other physiological stresses, such as hypercapnia, or differences in metabolic index parameters across clades not yet captured by existing (and limited) experimental data. Differences in

the latitude gradient of extinction when considering later Griesbachian taxonomic losses (Song *et al.*, 2020) may also point toward the importance of other stresses in causing extinctions after the initial pulse at the Permian-Triassic boundary itself.

Regardless of whether details of the Penn *et al.* (2018) findings are maintained following the collection of additional paleo-proxy, fossil, modeling, and experimental respirometry data, the principle of the approach is essential to use ancient episodes of climate change and extinction to test hypothesized extinction mechanisms and to inform projected biological responses to climate change in the twenty-first century. Simple, quantitative measures of habitat viability are required to translate between environmental changes determined from paleo-proxy data and biological responses observed from fossils. Biological traits that are conserved at high taxonomic levels, such as basic respiratory and circulatory anatomy, or are directly measurable from fossils, such as body size, are most amenable to inclusion in measures of habitat viability; but the influence of other variables can be determined by sampling from distributions constrained by measurements of living species.

Lessons from the Geological Oxygen Record for Modern Global Change

When attempting to draw lessons or analogies from the geologic past to modern and future global change, the major stumbling blocks are magnitude and timescale. The magnitude of both environmental change and marine extinction during the Big Five mass extinctions is simply not comparable to modern events—except under extreme scenarios of anthropogenic global change, we do not expect ~12 °C of tropical surface warming, near complete loss of oxygen in the ocean interior, and upward of 90% species extinction, such as characterized the Permian-Triassic boundary (Penn *et al.*, 2018; Penn and Deutsch, 2022). Conversely, while high-precision geochronology can only provide upper estimates for the timescale of ancient environmental change when such change was very rapid (*i.e.*, <50,000 years for the Permian-Triassic), and the geological record systematically under-estimates rates of climate change (Kemp *et al.*, 2015), there is no evidence that geologic forces come anywhere close to humanity's ability to rapidly transfer carbon from rock reservoirs to the atmosphere. Thus, modern organisms are likely facing a much lower-magnitude perturbation but a faster rate of change, which restricts the ability of natural feedback processes to mitigate environmental stresses. Studies of Pleistocene records (*e.g.*, Moffitt *et al.*, 2015; Salvatteci *et al.*, 2022) may provide more appropriate scales of oxygen or temperature change in terms of time and magnitude than the eye-catching Phanerozoic extinctions, although even here the timescale of change was still slower than the modern. Despite these issues, the geological record of oxygen changes (and temperature-dependent hypoxia) offers several important lessons for modern global change.

It is clear from the early Paleozoic record of oxygen and life that animal communities living under low atmospheric oxygen levels had very little aerobic buffer and were prone to rapid extinction from relatively modest changes in oxygen, temperature, or both. This has implications for the modern analog environment, specifically animals living in or near OMZs along continental margins. The geological observations provide a historical precedent consistent with observations from physiology (Wishner *et al.*, 2018) and sharp ecological thresholds in animal diversity or abundance with declining oxygen levels (Mullins *et al.*, 1985; Wishner *et al.*, 1990; Gooday *et al.*, 2009; Levin *et al.*, 2009; Sperling *et al.*, 2016). Together, these data from the ancient and modern Earth suggest that animals living in these environments today are likely to be especially vulnerable to loss of aerobic scope. Although such environments are often characterized as "muddy deserts," they host a mosaic of habitats and ecosystems with high regional diversity as well as increasingly important (and likely unsustainable) fisheries that have been developed as shallower-water species and stocks are overfished (Morato *et al.*, 2006; Levin and Sibuet, 2012). Perhaps equally important to consider with respect to future oxygen changes are impacts on the bioturbation activities of slope denizens. Continental margins are important sites of nutrient and carbon cycling (Berner, 1982), mediated in large part by animal bioturbators. While there have been biogeochemical studies of bioturbators in the modern ocean (*e.g.*, Aller and Aller, 1998), researchers have generally not directly investigated, at either the local scale or the global scale, the biogeochemical effects in a warming or deoxygenating ocean. In contrast, the action of bioturbators in the poorly oxygenated early Paleozoic has recently received increased scrutiny (albeit with varying modeling outcomes; Canfield and Farquhar, 2009; Boyle *et al.*, 2014; Tarhan *et al.*, 2015; van de Velde *et al.*, 2018). Most likely, the effects of global change on bioturbation are heterogenous and require nuance in global modeling efforts; for instance, biodiffusion mediates phosphorus burial, whereas bioirrigation recycles P to the water column and enhances productivity (Tarhan *et al.*, 2021). In any case, the lessons from and modeling approaches applied to the ancient low-oxygen world regarding bioturbation are likely to be useful in considering the biogeochemistry of our future oceans.

The most useful lesson from the ancient record (especially as a counter-point to climate change skeptics who claim that modern climate change could just be natural cycles or who question the link between CO_2 and climate change) is that over the past 400 million years, every time volcanic forces have injected massive amounts of CO_2 into the Earth system, we see evidence in the geologic record for global warming, ocean deoxygenation, ocean acidification, and widespread extinction of marine species. The timescales and magnitudes may be different, but the repeated response to natural carbon cycle perturbations is the same as that

observed today in response to anthropogenic fossil fuel combustion. Notably, biological recovery from such events takes hundreds of thousands to millions of years, as long as or longer than the timescale of return to pre-eruption environmental conditions. From a stressor perspective, these major extinction events all involve both deoxygenation and warming. Ecophysiological modeling of the Permian-Triassic extinction (Penn *et al.*, 2018) suggests that it was the synergistic combination of these two factors—with varying contribution by latitude—that best explains the pattern of extinction in the fossil record. This finding is consistent with recent meta-analyses suggesting that the combination of oxygen and temperature is by far the most detrimental stressor combination to marine invertebrates (Reddin *et al.*, 2020; Sampaio *et al.*, 2021) and highlights the importance of studying not just oxygen or temperature but, rather, temperature-dependent hypoxia.

Acknowledgments

EAS thanks Lisa Levin for the title suggestion and Lisa Levin and Andrew Knoll for their mentorship during a stimulating postdoctoral research experience studying oxygen and animals. Funding was provided to EAS, RGS, JAS, and JAM by National Science Foundation EAR-1922966 and to EAS and MID by an Environmental Venture Project grant from the Stanford Woods Institute for Environmental Studies. We thank Ben Black for photos of the Siberian Traps, Hunter Olson for help with figure preparation, and the Historical Geobiology Lab for feedback.

Literature Cited

Agić, H. 2021. Origin and early evolution of the eukaryotes: perspectives from the fossil record. Pp. 255–289 in *Prebiotic Chemistry and the Origin of Life*, A. Neubeck and S. McMahon, eds. Springer International, Cham, Switzerland.

Aller, R. C., and J. Y. Aller. 1998. The effect of biogenic irrigation intensity and solute exchange on diagenetic reaction rates in marine sediments. *J. Mar. Res.* **56:** 905–936.

Alroy, J. 2008. Dynamics of origination and extinction in the marine fossil record. *Proc. Natl. Acad. Sci. USA* **105:** 11536–11542.

Alroy, J. 2010. The shifting balance of diversity among major marine animal groups. *Science* **329:** 1191–1194.

Alroy, J., M. Aberhan, D. J. Bottjer, M. Foote, F. T. Fürsich, P. J. Harries, A. J. W. Hendy, S. M. Holland, L. C. Ivany, W. Kiessling *et al.* 2008. Phanerozoic trends in the global diversity of marine invertebrates. *Science* **321:** 97–100.

Alvarez, L. W., W. Alvarez, F. Asaro, and H. V. Michel. 1980. Extraterrestrial cause for the Cretaceous-Tertiary extinction. *Science* **208:** 1095–1108.

Beatty, T. W., J.-P. Zonneveld, and C. M. Henderson. 2008. Anomalously diverse Early Triassic ichnofossil assemblages in northwest Pangea: a case for a shallow-marine habitable zone. *Geology* **36:** 771–774.

Belcher, C. M., and J. C. McElwain. 2008. Limits for combustion in low O_2 redefine paleoatmospheric predictions for the Mesozoic. *Science* **321:** 1197–1200.

Bellefroid, E. J., A. V. S. Hood, P. F. Hoffman, M. D. Thomas, C. T. Reinhard, and N. J. Planavsky. 2018. Constraints on Paleoproterozoic atmospheric oxygen levels. *Proc. Natl. Acad. Sci. USA* **115:** 8104–8109.

Benton, M. J. 1995. Diversification and extinction in the history of life. *Science* **268:** 52–58.

Berner, R. A. 1982. Burial of organic carbon and pyrite sulfur in the modern ocean: its geochemical and environmental significance. *Am. J. Sci.* **282:** 451–473.

Berry, W. B., and P. Wilde. 1978. Progressive ventilation of the oceans: an explanation for the distribution of the lower Paleozoic black shales. *Am. J. Sci.* **278:** 257–275.

Black, B. A., L. T. Elkins-Tanton, M. C. Rowe, and I. U. Peate. 2012. Magnitude and consequences of volatile release from the Siberian Traps. *Earth Planet. Sci. Lett.* **317–318:** 363–373.

Blois, J. L., J. W. Williams, M. C. Fitzpatrick, S. T. Jackson, and S. Ferrier. 2013. Space can substitute for time in predicting climate-change effects on biodiversity. *Proc. Natl. Acad. Sci. USA* **110:** 9374–9379.

Boag, T. H., R. G. Stockey, L. E. Elder, P. M. Hull, and E. A. Sperling. 2018. Oxygen, temperature and the deep-marine stenothermal cradle of Ediacaran evolution. *Proc. R. Soc. B Biol. Sci.* **285:** 20181724.

Bond, D. P. G., and S. E. Grasby. 2017. On the causes of mass extinctions. *Palaeogeogr. Palaeoclimatol. Palaeoecol.* **478:** 3–29.

Bond, D. P. G., and P. B. Wignall. 2010. Pyrite framboid study of marine Permian-Triassic boundary sections: a complex anoxic event and its relationship to contemporaneous mass extinction. *Geol. Soc. Am. Bull.* **122:** 1265–1279.

Boscolo-Galazzo, F., K. A. Crichton, A. Ridgwell, E. M. Mawbey, B. S. Wade, and P. N. Pearson. 2021. Temperature controls carbon cycling and biological evolution in the ocean twilight zone. *Science* **371:** 1148–1152.

Boyle, R. A., T. W. Dahl, A. W. Dale, G. A. Shields-Zhou, M. Zhu, M. D. Brasier, D. E. Canfield, and T. M. Lenton. 2014. Stabilization of the coupled oxygen and phosphorus cycles by the evolution of bioturbation. *Nat. Geosci.* **7:** 671–676.

Breitburg, D., L. A. Levin, A. Oschlies, M. Grégoire, F. P. Chavez, D. J. Conley, V. Garçon, D. Gilbert, D. Gutiérrez, K. Isensee *et al.* 2018. Declining oxygen in the global ocean and coastal waters. *Science* **359:** eaam7240.

Brennecka, G. A., A. D. Herrmann, T. J. Algeo, and A. D. Anbar. 2011. Rapid expansion of oceanic anoxia immediately before the end-Permian mass extinction. *Proc. Natl. Acad. Sci. USA* **108:** 17631–17634.

Broadley, M. W., P. H. Barry, C. J. Ballentine, L. A. Taylor, and R. Burgess. 2018. End-Permian extinction amplified by plume-induced release of recycled lithospheric volatiles. *Nat. Geosci.* **11:** 682–687.

Burgess, S. D., and S. A. Bowring. 2015. High-precision geochronology confirms voluminous magmatism before, during, and after Earth's most severe extinction. *Sci. Adv.* **1:** e1500470.

Burgess, S. D., J. D. Muirhead, and S. A. Bowring. 2017. Initial pulse of Siberian Traps sills as the trigger of the end-Permian mass extinction. *Nat. Commun.* **8:** 164.

Butterfield, N. J. 2009a. Macroevolutionary turnover through the Ediacaran transition: ecological and biogeochemical implications. *Geol. Soc. Lond. Spec. Publ.* **326:** 55–66.

Butterfield, N. J. 2009b. Oxygen, animals and oceanic ventilation: an alternative view. *Geobiology* **7:** 1–7.

Butterfield, N. J. 2020. Constructional and functional anatomy of Ediacaran rangeomorphs. *Geol. Mag.* **159:** 1148–1159.

Calosi, P., H. M. Putnam, R. J. Twitchett, and F. Vermandele. 2019. Marine metazoan modern mass extinction: improving predictions by integrating fossil, modern, and physiological data. *Annu. Rev. Mar. Sci.* **11:** 369–390.

Campbell, I. H., G. K. Czamanske, V. A. Fedorenko, R. I. Hill, and V. Stepanov. 1992. Synchronism of the Siberian Traps and the Permian-Triassic boundary. *Science* **258:** 1760–1763.

Canfield, D. E. 1998. A new model for Proterozoic ocean chemistry. *Nature* **396:** 450–453.

Canfield, D. E. 2014. Proterozoic atmospheric oxygen. Pp. 197–216 in *Treatise on Geochemistry*, 2nd ed., H. D. Holland and K. K. Turekian, eds. Elsevier, Oxford.

Canfield, D. E., and J. Farquhar. 2009. Animal evolution, bioturbation, and the sulfate evolution of the oceans. *Proc. Natl. Acad. Sci. USA* **106:** 8123–8127.

Canfield, D. E., S. W. Poulton, A. H. Knoll, G. M. Narbonne, G. Ross, T. Goldberg, and H. Strauss. 2008. Ferruginous conditions dominated later Neoproterozoic deep-water chemistry. *Science* **321:** 949–952.

Cao, C., G. D. Love, L. E. Hays, S. A. Bowring, W. Wang, S. Shen, and R. E. Summons. 2009. Biogeochemical evidence for euxinic oceans and ecological disturbance presaging the end-Permian mass extinction event. *Earth Planet. Sci. Lett.* **281:** 188–201.

Chen, X., H.-F. Ling, D. Vance, G. A. Shields-Zhou, M. Zhu, S. W. Poulton, L. M. Och, S.-Y. Jiang, D. Li, L. Cremonese *et al.* 2015. Rise to modern levels of ocean oxygenation coincided with the Cambrian radiation of animals. *Nat. Commun.* **6:** 7142.

Chen, X., S. J. Romaniello, A. D. Herrmann, D. Hardisty, B. C. Gill, and A. D. Anbar. 2018. Diagenetic effects on uranium isotope fractionation in carbonate sediments from the Bahamas. *Geochim. Cosmochim. Acta* **237:** 294–311.

Clapham, M. E. 2019. Conservation evidence from climate-related stressors in the deep-time marine fossil record. *Philos. Trans. R. Soc. B Biol. Sci.* **374:** 20190223.

Clapham, M. E., and J. L. Payne. 2011. Acidification, anoxia, and extinction: a multiple logistic regression analysis of extinction selectivity during the Middle and Late Permian. *Geology* **39:** 1059–1062.

Clapham, M. E., and P. R. Renne. 2019. Flood basalts and mass extinctions. *Annu. Rev. Earth Planet. Sci.* **47:** 275–303.

Clarkson, M. O., R. A. Wood, S. W. Poulton, S. Richoz, R. J. Newton, S. A. Kasemann, F. Bowyer, and L. Krystyn. 2016. Dynamic anoxic ferruginous conditions during the end-Permian mass extinction and recovery. *Nat. Commun.* **7:** 12236.

Clarkson, M. O., C. H. Stirling, H. C. Jenkyns, A. J. Dickson, D. Porcelli, C. M. Moy, P. A. E. P. von Strandmann, I. R. Cooke, and T. M. Lenton. 2018. Uranium isotope evidence for two episodes of deoxygenation during Oceanic Anoxic Event 2. *Proc. Natl. Acad. Sci. USA* **115:** 2918–2923.

Clarkson, M. O., T. M. Lenton, M. B. Andersen, M.-L. Bagard, A. J. Dickson, and D. Vance. 2021. Upper limits on the extent of seafloor anoxia during the PETM from uranium isotopes. *Nat. Commun.* **12:** 399.

Cloud, P. C. 1976. Beginnings of biospheric evolution and their biogeochemical consequences. *Paleobiology* **2:** 351–387.

Cohen, P. A., and F. A. Macdonald. 2015. The Proterozoic record of eukaryotes. *Paleobiology* **41:** 610–632.

Cole, D. B., D. B. Mills, D. H. Erwin, E. A. Sperling, S. M. Porter, C. T. Reinhard, and N. J. Planavsky. 2020. On the co-evolution of surface oxygen levels and animals. *Geobiology* **18:** 260–281.

Cole, D. B., K. Ozaki, and C. T. Reinhard. 2022. Atmospheric oxygen abundance, marine nutrient availability, and organic carbon fluxes to the seafloor. *Glob. Biogeochem. Cycles* **36:** e2021GB007052.

Dahl, T. W., and S. K. Arens. 2020. The impacts of land plant evolution on Earth's climate and oxygenation state: an interdisciplinary review. *Chem. Geol.* **547:** 119665.

Dahl, T. W., E. U. Hammarlund, A. D. Anbar, D. P. G. Bond, B. C. Gill, G. W. Gordon, A. H. Knoll, A. T. Nielsen, N. H. Schovsbo, and D. E. Canfield. 2010. Devonian rise in atmospheric oxygen correlated to the radiation of terrestrial plants and large

predatory fish. *Proc. Natl. Acad. Sci. USA* **107:** 17911–17915.

Dahl, T. W., M.-L. Siggaard-Andersen, N. H. Schovsbo, D. O. Persson, S. Husted, I. W. Hougård, A. J. Dickson, K. Kjær, and A. T. Nielsen. 2019. Brief oxygenation events in locally anoxic oceans during the Cambrian solves the animal breathing paradox. *Sci. Rep.* **9:** 1–9.

Deutsch, C., A. Ferrel, B. Seibel, H.-O. Pörtner, and R. B. Huey. 2015. Climate change tightens a metabolic constraint on marine habitats. *Science* **348:** 1132–1135.

Deutsch, C., J. L. Penn, and B. Seibel. 2020. Metabolic trait diversity shapes marine biogeography. *Nature* **585:** 557–562.

Diamond, C. W., and T. W. Lyons. 2018. Mid-Proterozoic redox evolution and the possibility of transient oxygenation events. *Emerg. Top. Life Sci.* **2:** 235–245.

Dohrmann, M., and G. Wörheide. 2017. Dating early animal evolution using phylogenomic data. *Sci. Rep.* **7:** 3599.

Droser, M. L., D. J. Bottjer, P. M. Sheehan, and G. R. McGhee, Jr. 2000. Decoupling of taxonomic and ecologic severity of Phanerozoic marine mass extinctions. *Geology* **28:** 675–678.

Dzik, J. 2007. The Verdun syndrome: simultaneous origin of protective armour and infaunal shelters at the Precambrian-Cambrian transition. *Geol. Soc. Lond. Spec. Publ.* **286:** 405–414.

Edwards, C. T., M. R. Saltzman, D. L. Royer, and D. A. Fike. 2017. Oxygenation as a driver of the Great Ordovician Biodiversification Event. *Nat. Geosci.* **10:** 925–929.

Elkins-Tanton, L. T., S. E. Grasby, B. A. Black, R. V. Veselovskiy, O. H. Ardakani, and F. Goodarzi. 2020. Field evidence for coal combustion links the 252 Ma Siberian Traps with global carbon disruption. *Geology* **48:** 986–991.

Elrick, M., V. Polyak, T. J. Algeo, S. Romaniello, Y. Asmerom, A. D. Herrmann, A. D. Anbar, L. Zhao, and Z.-Q. Chen. 2017. Global-ocean redox variation during the middle-late Permian through Early Triassic based on uranium isotope and Th/U trends of marine carbonates. *Geology* **45:** 163–166.

Ernst, R. E., and N. Youbi. 2017. How large igneous provinces affect global climate, sometimes cause mass extinctions, and represent natural markers in the geological record. *Palaeogeogr. Palaeoclimatol. Palaeoecol.* **478:** 30–52.

Ernst, R. E., D. P. G. Bond, and S. H. Zhang. 2020. Influence of large igneous provinces. Pp. 345–356 in *Geologic Time Scale 2020*, F. M. Gradstein, J. G. Ogg, M. D. Schmitz, and G. M. Ogg, eds. Elsevier, Oxford.

Erwin, D. H. 1993. *The Great Paleozoic Crisis: Life and Death in the Permian*. Columbia University Press, New York.

Erwin, D. H., M. Laflamme, S. M. Tweedt, E. A. Sperling, D. Pisani, and K. J. Peterson. 2011. The Cambrian conundrum: early divergence and later ecological success in the early history of animals. *Science* **334:** 1091–1097.

Fakhraee, M., N. J. Planavsky, and C. T. Reinhard. 2020. The role of environmental factors in the long-term evolution of the marine biological pump. *Nat. Geosci.* **13:** 812–816.

Farquhar, J., H. Bao, and M. Thiemens. 2000. Atmospheric influence of earth's earliest sulfur cycle. *Science* **289:** 756–758.

Foote, M. 2003. Origination and extinction through the Phanerozoic: a new approach. *J. Geol.* **111:** 125–148.

Foster, W. J., G. Ayzel, J. Münchmeyer, T. Rettelbach, N. H. Kitzmann, T. T. Isson, M. Mutti, and M. Aberhan. 2022. Machine learning identifies ecological selectivity patterns across the end-Permian mass extinction. *Paleobiology* **48:** 357–371.

Ganino, C., and N. T. Arndt. 2009. Climate changes caused by degassing of sediments during the emplacement of large igneous provinces. *Geology* **37:** 323–326.

Garcia, H., K. Weathers, C. Paver, I. Smolyar, T. Boyer, R. Locarnini, M. Zweng, A. Mishonov, O. Baranova, D. Seidov *et al.* 2019. *World Ocean Atlas 2018*, Vol. 3, *Dissolved Oxygen, Apparent Oxygen Utilization, and Dissolved Oxygen Saturation*. NOAA National Centers for Environmental Information, Silver Springs, MD.

Gill, B. C., T. W. Dahl, E. U. Hammarlund, M. A. LeRoy, G. W. Gordon, D. E. Canfield, A. D. Anbar, and T. W. Lyons. 2021. Redox dynamics of later Cambrian oceans. *Palaeogeogr. Palaeoclimatol. Palaeoecol.* **581:** 110623.

Gilleaudeau, G., S. Romaniello, G. Luo, A. Kaufman, F. Zhang, R. Klaebe, L. Kah, K. Azmy, J. Bartley, W. Zheng *et al.* 2019. Uranium isotope evidence for limited euxinia in mid-Proterozoic oceans. *Earth Planet. Sci. Lett.* **521:** 150–157.

Goldberg, S. L., T. M. Present, S. Finnegan, and K. D. Bergmann. 2021. A high-resolution record of early Paleozoic climate. *Proc. Natl. Acad. Sci. USA* **118:** e2013083118.

Gooday, A. J., L. A. Levin, A. A. da Silva, B. J. Bett, G. Cowie, D. Dissard, J. D. Gage, D. J. Hughes, R. Jeffreys, P. A. Lamont *et al.* 2009. Faunal responses to oxygen gradients on the Pakistan margin: a comparison of foraminiferans, macrofauna and megafauna. *Deep-Sea Res. Pt. II Top. Stud. Oceanogr.* **56:** 488–502.

Grasby, S. E., H. Sanei, and B. Beauchamp. 2011. Catastrophic dispersion of coal fly ash into oceans during the latest Permian extinction. *Nat. Geosci.* **4:** 104–107.

Grice, K., C. Cao, G. D. Love, M. E. Bottcher, R. J. Twitchett, E. Grosjean, R. E. Summons, S. C. Turgeon, W. Dunning, and Y. Jin. 2005. Photic zone euxinia during the Permian-Triassic superanoxic event. *Science* **307:** 706–709.

Guilbaud, R., S. W. Poulton, N. J. Butterfield, M. Zhu, and G. A. Shields-Zhou. 2015. A global transition to ferruginous conditions in the early Neoproterozoic oceans. *Nat. Geosci.* **8:** 466–470.

Hardisty, D. S., Z. Lu, N. J. Planavsky, A. Bekker, P. Philippot, X. Zhou, and T. W. Lyons. 2014. An iodine record of Paleoproterozoic surface ocean oxygenation. *Geology* **42:** 619–622.

Harnik, P. G., H. K. Lotze, S. C. Anderson, Z. V. Finkel, S. Finnegan, D. R. Lindberg, L. H. Liow, R. Lockwood, C. R. McClain, J. L. McGuire *et al.* 2012. Extinctions in ancient and modern seas. *Trends Ecol. Evol.* **27:** 608–617.

Hodgskiss, M. S. W., and E. A. Sperling. 2022. A prolonged, two-step oxygenation of Earth's early atmosphere: support from confidence intervals. *Geology* **50:** 158–162.

Hofmann, A., E. Peltzer, P. Walz, and P. Brewer. 2011. Hypoxia by degrees: establishing definitions for a changing ocean. *Deep-Sea Res. Pt. I Oceanogr. Res. Pap.* **58:** 1212–1226.

Hu, D., M. Li, X. Zhang, A. V. Turchyn, Y. Gong, and Y. Shen. 2020. Large mass-independent sulphur isotope anomalies link stratospheric volcanism to the Late Ordovician mass extinction. *Nat. Commun.* **11:** 2297.

Hull, P. M., A. Bornemann, D. E. Penman, M. J. Henehan, R. D. Norris, P. A. Wilson, P. Blum, L. Alegret, S. J. Batenburg, P. R. Bown *et al.* 2020. On impact and volcanism across the Cretaceous-Paleogene boundary. *Science* **367:** 266–272.

Hülse, D., K. V. Lau, S. J. van de Velde, S. Arndt, K. M. Meyer, and A. Ridgwell. 2021. End-Permian marine extinction due to temperature-driven nutrient recycling and euxinia. *Nat. Geosci.* **14:** 862–867.

Isozaki, Y. 1997. Permo-Triassic boundary superanoxia and stratified superocean: records from lost deep sea. *Science* **276:** 235–238.

Joachimski, M. M., X. Lai, S. Shen, H. Jiang, G. Luo, B. Chen, J. Chen, and Y. Sun. 2012. Climate warming in the latest Permian and the Permian-Triassic mass extinction. *Geology* **40:** 195–198.

Joachimski, M. M., A. S. Alekseev, A. Grigoryan, and Y. A. Gatovsky. 2019. Siberian Trap volcanism, global warming and the Permian-Triassic mass extinction: new insights from Armenian Permian-Triassic sections. *Geol. Soc. Am. Bull.* **132:** 427–443.

Jones, D. S., A. M. Martini, D. A. Fike, and K. Kaiho. 2017. A volcanic trigger for the Late Ordovician mass extinction? Mercury data from south China and Laurentia. *Geology* **45:** 631–634.

Jones, T. P., and W. G. Chaloner. 1991. Fossil charcoal, its recognition and palaeoatmospheric significance. *Palaeogeogr. Palaeoclimatol. Palaeoecol.* **97:** 39–50.

Jost, A. B., A. Bachan, B. van de Schootbrugge, K. V. Lau, K. L. Weaver, K. Maher, and J. L. Payne. 2017. Uranium isotope evidence for an expansion of marine anoxia during the end-Triassic extinction. *Geochem. Geophys. Geosyst.* **18:** 3093–3108.

Kasbohm, J., B. Schoene, and S. Burgess. 2021. Radiometric constraints on the timing, tempo, and effects of large igneous province emplacement. Pp. 27–82 in *Large Igneous Provinces*, R. E. Ernst, A. J. Dickson, and A. Bekker, eds. American Geophysical Union, Washington, DC.

Kemp, D. B., K. Eichenseer, and W. Kiessling. 2015. Maximum rates of climate change are systematically underestimated in the geological record. *Nat. Commun.* **6:** 8890.

Kendall, B. 2021. Recent advances in geochemical paleooxybarometers. *Annu. Rev. Earth Planet. Sci.* **49:** 399–433.

Kendall, B., T. W. Dahl, and A. D. Anbar. 2017. Good golly, why moly? The stable isotope geochemistry of molybdenum. Pp. 683–732 in *Non-Traditional Stable Isotopes*, F.-Z. Teng, J. Watkins, and N. Dauphas, eds. De Gruyter, Berlin.

Kiessling, W., and C. Simpson. 2011. On the potential for ocean acidification to be a general cause of ancient reef crises. *Glob. Change Biol.* **17:** 56–67.

Kipp, M. A., and F. L. H. Tissot. 2022. Inverse methods for consistent quantification of seafloor anoxia using uranium isotope data from marine sediments. *Earth Planet. Sci. Lett.* **577:** 117240.

Knoll, A. H. 2013. Systems paleobiology. *Geol. Soc. Am. Bull.* **125:** 3–13.

Knoll, A. H., R. K. Bambach, D. E. Canfield, and J. P. Grotzinger. 1996. Comparative earth history and Late Permian mass extinction. *Science* **273:** 452–457.

Knoll, A. H., R. K. Bambach, J. L. Payne, S. Pruss, and W. Fischer. 2007. Paleophysiology and end-Permian mass extinction. *Earth Planet. Sci. Lett.* **256:** 295–313.

Kocsis, Á. T., C. J. Reddin, J. Alroy, and W. Kiessling. 2019. The R package divDyn for quantifying diversity dynamics using fossil sampling data. *Methods Ecol. Evol.* **10:** 735–743.

Krause, A. J., B. J. W. Mills, S. Zhang, N. J. Planavsky, T. M. Lenton, and S. W. Poulton. 2018. Stepwise oxygenation of the Paleozoic atmosphere. *Nat. Commun.* **9:** 1–10.

Kump, L. R. 2008. The rise of atmospheric oxygen. *Nature* **451:** 277–278.

Lau, K. V., K. Maher, D. Altiner, B. M. Kelley, L. R. Kump, D. J. Lehrmann, J. C. Silva-Tamayo, K. L. Weaver, M. Yu, and J. L. Payne. 2016. Marine anoxia and delayed Earth system recovery after the

end-Permian extinction. *Proc. Natl. Acad. Sci. USA* **113:** 2360–2365.

Lenton, T. M., S. J. Daines, and B. J. W. Mills. 2018. COPSE reloaded: an improved model of biogeochemical cycling over Phanerozoic time. *Earth-Sci. Rev.* **178:** 1–28.

Levin, L. A. 2018. Manifestation, drivers, and emergence of open ocean deoxygenation. *Annu. Rev. Mar. Sci.* **10:** 229–260.

Levin, L. A., and M. Sibuet. 2012. Understanding continental margin biodiversity: a new imperative. *Annu. Rev. Mar. Sci.* **4:** 79–112.

Levin, L. A., C. R. Whitcraft, G. F. Mendoza, J. P. Gonzalez, and G. Cowie. 2009. Oxygen and organic matter thresholds for benthic faunal activity on the Pakistan margin oxygen minimum zone (700–1100 m). *Deep-Sea Res. Pt. II Top. Stud. Oceanogr.* **56:** 449–471.

Leys, S. P., and A. S. Kahn. 2018. Oxygen and the energetic requirements of the first multicellular animals. *Integr. Comp. Biol.* **58:** 666–676.

Liu, X.-M., L. C. Kah, A. H. Knoll, H. Cui, C. Wang, A. Bekker, and R. M. Hazen. 2021. A persistently low level of atmospheric oxygen in Earth's middle age. *Nat. Commun.* **12:** 351.

Lu, W., A. Ridgwell, E. Thomas, D. S. Hardisty, G. Luo, T. J. Algeo, M. R. Saltzman, B. C. Gill, Y. Shen, H.-F. Ling *et al.* 2018. Late inception of a resiliently oxygenated upper ocean. *Science* **361:** 174–177.

Lu, Z., B. A. A. Hoogakker, C.-D. Hillenbrand, X. Zhou, E. Thomas, K. M. Gutchess, W. Lu, L. Jones, and R. E. M. Rickaby. 2016. Oxygen depletion recorded in upper waters of the glacial Southern Ocean. *Nat. Commun.* **7:** 11146.

Lyons, T. W., C. T. Reinhard, and N. J. Planavsky. 2014. The rise of oxygen in Earth's early ocean and atmosphere. *Nature* **506:** 307–315.

Marenco, P. J., K. R. Martin, K. N. Marenco, and D. C. Barber. 2016. Increasing global ocean oxygenation and the Ordovician radiation: insights from Th/U of carbonates from the Ordovician of western Utah. *Palaeogeogr. Palaeoclimatol. Palaeoecol.* **458:** 77–84.

Marshall, C. R. 2006. Explaining the Cambrian "explosion" of animals. *Annu. Rev. Earth Planet. Sci.* **34:** 355–384.

McCormick, L. R., L. A. Levin, and N. W. Oesch. 2019. Vision is highly sensitive to oxygen availability in marine invertebrate larvae. *J. Exp. Biol.* **222:** jeb.200899.

Mentel, M., M. Röttger, S. Leys, A. G. M. Tielens, and W. F. Martin. 2014. Of early animals, anaerobic mitochondria, and a modern sponge. *BioEssays* **36:** 924–932.

Meyer, K. M., A. Ridgwell, and J. L. Payne. 2016. The influence of the biological pump on ocean chemistry: implications for long-term trends in marine redox chemistry, the global carbon cycle, and the evolution of marine animal ecosystems. *Geobiology* **14:** 207–219.

Micaroni, V., F. Strano, R. McAllen, L. Woods, J. Turner, L. Harman, and J. J. Bell. 2021. Adaptive strategies of sponges to deoxygenated oceans. *Glob. Change Biol.* **28:** 1972–1989.

Mills, D. B., and D. E. Canfield. 2014. Oxygen and animal evolution: Did a rise of atmospheric oxygen "trigger" the origin of animals? *BioEssays* **36:** 1145–1155.

Mills, D. B., L. M. Ward, C. Jones, B. Sweeten, M. Forth, A. H. Treusch, and D. E. Canfield. 2014. Oxygen requirements of the earliest animals. *Proc. Natl. Acad. Sci. USA* **111:** 4168–4172.

Mills, D. B., W. R. Francis, S. Vargas, M. Larsen, C. P. Elemans, D. E. Canfield, and G. Wörheide. 2018. The last common ancestor of animals lacked the HIF pathway and respired in low-oxygen environments. *eLife* **7:** e31176.

Moffitt, S. E., T. M. Hill, P. D. Roopnarine, and J. P. Kennett. 2015. Response of seafloor ecosystems to abrupt global climate change. *Proc. Natl. Acad. Sci. USA* **112:** 4684–4689.

Morato, T., R. Watson, T. J. Pitcher, and D. Pauly. 2006. Fishing down the deep. *Fish Fish.* **7:** 24–34.

Müller, M., M. Mentel, J. J. van Hellemond, K. Henze, C. Woehle, S. B. Gould, R.-Y. Yu, M. van der Giezen, A. G. M. Tielens, and W. F. Martin. 2012. Biochemistry and evolution of anaerobic energy metabolism in eukaryotes. *Microbiol. Mol. Biol. Rev.* **76:** 444–495.

Mullins, H. T., J. B. Thompson, K. McDougall, and T. L. Vercoutere. 1985. Oxygen-minimum zone edge effects: evidence from the central California coastal upwelling system. *Geology* **13:** 491–494.

Nursall, J. R. 1959. Oxygen as a prerequisite to the origin of the Metazoa. *Nature* **183:** 1170–1172.

Ogden, D. E., and N. H. Sleep. 2012. Explosive eruption of coal and basalt and the end-Permian mass extinction. *Proc. Natl. Acad. Sci. USA* **109:** 59–62.

Ozaki, K., and E. Tajika. 2013. Biogeochemical effects of atmospheric oxygen concentration, phosphorus weathering, and sea-level stand on oceanic redox chemistry: implications for greenhouse climates. *Earth Planet. Sci. Lett.* **373:** 129–139.

Paleobiology Database. 2022. Revealing the history of life. [Online]. Available: https://paleobiodb.org [2022, September 12].

Parker, A. 2003. *In The Blink of an Eye: How Vision Sparked the Big Bang of Evolution*. Perseus, Cambridge, MA.

Pavlov, A., and J. Kasting. 2002. Mass-independent fractionation of sulfur isotopes in Archean sediments: strong evidence for an anoxic Archean atmosphere. *Astrobiology* **2:** 27–41.

Payne, J. L., and M. E. Clapham. 2012. End-Permian mass extinction in the oceans: an ancient analog for the twenty-first century? *Annu. Rev. Earth Planet. Sci.* **40:** 89–111.

Payne, J. L., D. J. Lehrmann, J. Wei, and A. H. Knoll. 2006. The pattern and timing of biotic recovery from the End-Permian extinction on the Great Bank of Guizhou, Guizhou Province, China. *Palaios* **21:** 63–85.

Payne, J. L., A. Bachan, N. A. Heim, P. M. Hull, and M. L. Knope. 2020. The evolution of complex life and the stabilization of the Earth system. *Interface Focus* **10:** 20190106.

Penn, J. L., and C. Deutsch. 2022. Avoiding ocean mass extinction from climate warming. *Science* **376:** 524–526.

Penn, J. L., C. Deutsch, J. L. Payne, and E. A. Sperling. 2018. Temperature-dependent hypoxia explains biogeography and severity of end-Permian marine mass extinction. *Science* **362:** eaat1327.

Peterson, K. J., M. A. McPeek, and D. A. D. Evans. 2005. Tempo and mode of early animal evolution: inferences from rocks, Hox, and molecular clocks. *Paleobiology* **31(suppl.):** 36–55.

Petit, J. R., J. Jouzel, D. Raynaud, N. I. Barkov, G. Delaygue, M. Delmotte, V. M. Kotlyakov, M. Legrand, V. Y. Lipenkov, C. Lorius *et al.* 1999. Climate and atmospheric history of the past 420,000 years from the Vostok ice core, Antarctica. *Nature* **399:** 429–436.

Pimentel-Galvan, M., K. V. Lau, K. Maher, T. Mukerji, D. J. Lehrmann, D. Altiner, and J. L. Payne. 2022. Duration and intensity of End-Permian marine anoxia. *Geochem. Geophys. Geosyst.* **23:** e2021GC010130.

Planavsky, N. J., P. McGoldrick, C. T. Scott, C. Li, C. T. Reinhard, A. E. Kelly, X. Chu, A. Bekker, G. D. Love, and T. W. Lyons. 2011. Widespread iron-rich conditions in the mid-Proterozoic ocean. *Nature* **477:** 448–451.

Planavsky, N. J., D. B. Cole, T. T. Isson, C. T. Reinhard, P. W. Crockford, N. D. Sheldon, and T. W. Lyons. 2018. A case for low atmospheric oxygen levels during Earth's middle history. *Emerg. Top. Life Sci.* **2:** 149–159.

Pohl, A., D. A. T. Harper, Y. Donnadieu, G. Le Hir, E. Nardin, and T. Servais. 2018. Possible patterns of marine primary productivity during the Great Ordovician Biodiversification Event. *Lethaia* **51:** 187–197.

Pörtner, H.-O. 2010. Oxygen- and capacity-limitation of thermal tolerance: a matrix for integrating climate-related stressor effects in marine ecosystems. *J. Exp. Biol.* **213:** 881–893.

Poulton, S. W. 2021. *The Iron Speciation Paleoredox Proxy*. Cambridge University Press, Cambridge.

Poulton, S. W., and D. E. Canfield. 2011. Ferruginous conditions: a dominant feature of the ocean through Earth's history. *Elements* **7:** 107–112.

Poulton, S. W., A. Bekker, V. M. Cumming, A. L. Zerkle, D. E. Canfield, and D. T. Johnston. 2021. A 200-million-year delay in permanent atmospheric oxygenation. *Nature* **592:** 232–236.

Raup, D. M., and J. J. Sepkoski. 1982. Mass extinctions in the marine fossil record. *Science* **215:** 1501–1503.

Reddin, C. J., P. S. Nätscher, Á. T. Kocsis, H.-O. Pörtner, and W. Kiessling. 2020. Marine clade sensitivities to climate change conform across timescales. *Nat. Clim. Change* **10:** 249–253.

Reichow, M. K., M. S. Pringle, A. I. Al'Mukhamedov, M. B. Allen, V. L. Andreichev, M. M. Buslov, C. E. Davies, G. S. Fedoseev, J. G. Fitton, S. Inger *et al.* 2009. The timing and extent of the eruption of the Siberian Traps large igneous province: implications for the end-Permian environmental crisis. *Earth Planet. Sci. Lett.* **277:** 9–20.

Reinhard, C. T., and N. J. Planavsky. 2022. The history of ocean oxygenation. *Annu. Rev. Mar. Sci.* **14:** 331–353.

Reinhard, C. T., N. J. Planavsky, S. L. Olson, T. W. Lyons, and D. H. Erwin. 2016. Earth's oxygen cycle and the evolution of animal life. *Proc. Natl. Acad. Sci. USA* **113:** 8933–8938.

Reinhard, C. T., N. J. Planavsky, B. A. Ward, G. D. Love, G. Le Hir, and A. Ridgwell. 2020. The impact of marine nutrient abundance on early eukaryotic ecosystems. *Geobiology* **18:** 139–151.

Renne, P. R., and A. R. Basu. 1991. Rapid eruption of the Siberian Traps flood basalts at the Permo-Triassic boundary. *Science* **253:** 176–179.

Rhoads, D. C., and J. W. Morse. 1971. Evolutionary and ecologic significance of oxygen-deficient marine basins. *Lethaia* **4:** 413–428.

Ridgwell, A., J. C. Hargreaves, N. R. Edwards, J. D. Annan, T. M. Lenton, R. Marsh, A. Yool, and A. Watson. 2007. Marine geochemical data assimilation in an efficient earth system model of global biogeochemical cycling. *Biogeosciences* **4:** 87–104.

Runnegar, B. 1982a. The Cambrian explosion: animals or fossils? *J. Geol. Assoc. Aust.* **29:** 395–411.

Runnegar, B. 1982b. Oxygen requirements, biology and phylogenetic significance of the late Precambrian worm *Dickinsonia*, and the evolution of the burrowing habit. *Alcheringa* **6:** 223–239.

Saltzman, M. R., C. T. Edwards, J. M. Adrain, and S. R. Westrop. 2015. Persistent oceanic anoxia and elevated extinction rates separate the Cambrian and Ordovician radiations. *Geology* **43:** 807–810.

Salvatteci, R., R. R. Schneider, E. Galbraith, D. Field, T. Blanz, T. Bauersachs, X. Crosta, P. Martinez, V. Echevin, F. Scholz *et al.* 2022. Smaller fish species in a warm and oxygen-poor Humboldt Current system. *Science* **375:** 101–104.

Sampaio, E., C. Santos, I. C. Rosa, V. Ferreira, H.-O. Pörtner, C. M. Duarte, L. A. Levin, and R. Rosa. 2021. Impacts of hypoxic events surpass those of future ocean warming and acidification. *Nat. Ecol. Evol.* **5:** 311–321.

Schobben, M., W. J. Foster, A. R. N. Sleveland, V. Zuchuat, H. H. Svensen, S. Planke, D. P. G. Bond, F. Marcelis, R. J. Newton, P. B. Wignall *et al.* 2020. A nutrient control on marine anoxia during the end-Permian mass extinction. *Nat. Geosci.* **13:** 640–646.

Schoene, B., K. M. Samperton, M. P. Eddy, G. Keller, T. Adatte, S. A. Bowring, S. F. R. Khadri, and B. Gertsch. 2015. U-Pb geochronology of the Deccan Traps and relation to the end-Cretaceous mass extinction. *Science* **347:** 182–184.

Scott, A. C., and I. J. Glasspool. 2006. The diversification of Paleozoic fire systems and fluctuations in atmospheric oxygen concentration. *Proc. Natl. Acad. Sci. USA* **103:** 10861–10865.

Sepkoski, J. J. 1981. A factor analytic description of the Phanerozoic marine fossil record. *Paleobiology* **7:** 36–53.

Shen, Y., A. H. Knoll, and M. R. Walter. 2003. Evidence for low sulphate and anoxia in a mid-Proterozoic marine basin. *Nature* **423:** 632–635.

Sobolev, S. V., A. V. Sobolev, D. V. Kuzmin, N. A. Krivolutskaya, A. G. Petrunin, N. T. Arndt, V. A. Radko, and Y. R. Vasiliev. 2011. Linking mantle plumes, large igneous provinces and environmental catastrophes. *Nature* **477:** 312–316.

Song, H., H. Song, T. J. Algeo, J. Tong, S. J. Romaniello, Y. Zhu, D. Chu, Y. Gong, and A. D. Anbar. 2017. Uranium and carbon isotopes document global-ocean redox-productivity relationships linked to cooling during the Frasnian-Famennian mass extinction. *Geology* **45:** 887–890.

Song, H., S. Huang, E. Jia, X. Dai, P. B. Wignall, and A. M. Dunhill. 2020. Flat latitudinal diversity gradient caused by the Permian-Triassic mass extinction. *Proc. Natl. Acad. Sci. USA* **117:** 17578–17583.

Sperling, E. A., and R. G. Stockey. 2018. The temporal and environmental context of early animal evolution: considering all the ingredients of an "explosion." *Integr. Comp. Biol.* **58:** 605–622.

Sperling, E. A., C. A. Frieder, A. V. Raman, P. R. Girguis, L. A. Levin, and A. H. Knoll. 2013a. Oxygen, ecology, and the Cambrian radiation of animals. *Proc. Natl. Acad. Sci. USA* **110:** 13446–13451.

Sperling, E. A., G. P. Halverson, A. H. Knoll, F. A. Macdonald, and D. T. Johnston. 2013b. A basin redox transect at the dawn of animal life. *Earth Planet. Sci. Lett.* **371:** 143–155.

Sperling, E. A., A. H. Knoll, and P. R. Girguis. 2015a. The ecological physiology of Earth's second oxygen revolution. *Annu. Rev. Ecol. Evol. Syst.* **46:** 215–235.

Sperling, E. A., C. J. Wolock, A. S. Morgan, B. C. Gill, M. Kunzmann, G. P. Halverson, F. A. Macdonald, A. H. Knoll, and D. T. Johnston. 2015b. Statistical analysis of iron geochemical data suggests limited late Proterozoic oxygenation. *Nature* **523:** 451–454.

Sperling, E. A., C. A. Frieder, and L. A. Levin. 2016. Biodiversity response to natural gradients of multiple stressors on continental margins. *Proc. R. Soc. B Biol. Sci.* **283:** 20160637.

Sperling, E. A., U. Balthasar, and C. B. Skovsted. 2018. On the edge of exceptional preservation: insights into the role of redox state in Burgess Shale-type taphonomic windows from the Mural Formation, Alberta, Canada. *Emerg. Top. Life Sci.* **2:** 311–323.

Sperling, E. A., M. J. Melchin, T. Fraser, R. G. Stockey, U. C. Farrell, L. Bhajan, T. N. Brunoir, D. B. Cole, B. C. Gill, A. Lenz *et al.* 2021. A long-term record of early to mid-Paleozoic marine redox change. *Sci. Adv.* **7:** eabf4382.

Stockey, R. G., D. B. Cole, N. J. Planavsky, D. K. Loydell, J. Fryda, and E. A. Sperling. 2020. Persistent global marine euxinia in the early Silurian. *Nat. Commun.* **11:** 1804.

Stockey, R. G., A. Pohl, A. Ridgwell, S. Finnegan, and E. A. Sperling. 2021. Decreasing Phanerozoic extinction intensity as a consequence of Earth surface oxygenation and metazoan ecophysiology. *Proc. Natl. Acad. Sci. USA* **118:** e2101900118.

Sun, Y., M. M. Joachimski, P. B. Wignall, C. Yan, Y. Chen, H. Jiang, L. Wang, and X. Lai. 2012. Lethally hot temperatures during the Early Triassic greenhouse. *Science* **338:** 366–370.

Svensen, H., S. Planke, A. G. Polozov, N. Schmidbauer, F. Corfu, Y. Y. Podladchikov, and B. Jamtveit. 2009. Siberian gas venting and the end-Permian environmental crisis. *Earth Planet. Sci. Lett.* **277:** 490–500.

Tarhan, L. G., M. L. Droser, N. J. Planavsky, and D. T. Johnston. 2015. Protracted development of bioturbation through the early Palaeozoic Era. *Nat. Geosci.* **8:** 865–869.

Tarhan, L. G., M. Zhao, and N. J. Planavsky. 2021. Bioturbation feedbacks on the phosphorus cycle. *Earth Planet. Sci. Lett.* **566:** 116961.

Them, T. R., B. C. Gill, A. H. Caruthers, A. M. Gerhardt, D. R. Gröcke, T. W. Lyons, S. M. Marroquín, S. G. Nielsen, J. P. T. Alexandre, and J. D. Owens. 2018. Thallium isotopes reveal protracted anoxia during the Toarcian (Early Jurassic) associated with volcanism, carbon burial, and mass extinction. *Proc. Natl. Acad. Sci. USA* **115:** 6596–6601.

Towe, K. M. 1970. Oxygen-collagen priority and the early metazoan fossil record. *Proc. Natl. Acad. Sci. USA* **65:** 781–788.

Tribovillard, N., T. J. Algeo, F. Baudin, and A. Riboulleau. 2012. Analysis of marine environmental

conditions based on molybdenum-uranium covariation: applications to Mesozoic paleoceanography. *Chem. Geol.* **324–325:** 46–58.

Urey, H. C. 1952. *The Planets: Their Origin and Development*. Yale University Press, New Haven, CT.

van de Velde, S., B. J. W. Mills, F. J. R. Meysman, T. M. Lenton, and S. W. Poulton. 2018. Early Palaeozoic ocean anoxia and global warming driven by the evolution of shallow burrowing. *Nat. Commun.* **9:** 2554.

Wallace, M. W., A. Hood, A. Shuster, A. Greig, N. J. Planavsky, and C. Reed. 2017. Oxygenation history of the Neoproterozoic to early Phanerozoic and the rise of land plants. *Earth Planet. Sci. Lett.* **466:** 12–19.

Watson, A., J. E. Lovelock, and L. Margulis. 1978. Methanogenesis, fires and the regulation of atmospheric oxygen. *Biosystems* **10:** 293–298.

Wei, G.-Y., N. J. Planavsky, L. G. Tarhan, X. Chen, W. Wei, D. Li, and H.-F. Ling. 2018. Marine redox fluctuation as a potential trigger for the Cambrian explosion. *Geology* **46:** 587–590.

White, D. A., M. Elrick, S. Romaniello, and F. Zhang. 2018. Global seawater redox trends during the Late Devonian mass extinction detected using U isotopes of marine limestones. *Earth Planet. Sci. Lett.* **503:** 68–77.

Wignall, P. B., and A. Hallam. 1992. Anoxia as a cause of the Permian/Triassic mass extinction: facies evidence from northern Italy and the western United States. *Palaeogeogr. Palaeoclimatol. Palaeoecol.* **93:** 21–46.

Wignall, P. B., and R. J. Twitchett. 1996. Oceanic anoxia and the end Permian mass extinction. *Science* **272:** 1155–1158.

Wildman, R. A., Jr., L. J. Hickey, M. B. Dickinson, R. A. Berner, J. M. Robinson, M. Dietrich, R. H. Essenhigh, and C. B. Wildman. 2004. Burning of forest materials under late Paleozoic high atmospheric oxygen levels. *Geology* **32:** 457–460.

Wishner, K., L. Levin, M. Gowing, and L. Mullineaux. 1990. Involvement of the oxygen minimum in benthic zonation on a deep seamount. *Nature* **346:** 57–59.

Wishner, K. F., B. A. Seibel, C. Roman, C. Deutsch, D. Outram, C. T. Shaw, M. A. Birk, K. A. S. Mislan, T. J. Adams, D. Moore *et al.* 2018. Ocean deoxygenation and zooplankton: very small oxygen differences matter. *Sci. Adv.* **4:** eaau5180.

Wood, R., A. G. Liu, F. Bowyer, P. R. Wilby, F. S. Dunn, C. G. Kenchington, J. F. H. Cuthill, E. G. Mitchell, and A. Penny. 2019. Integrated records of environmental change and evolution challenge the Cambrian explosion. *Nat. Ecol. Evol.* **3:** 528–538.

Yan, Y., E. J. Brook, A. V. Kurbatov, J. P. Severinghaus, and J. A. Higgins. 2021. Ice core evidence for atmospheric oxygen decline since the Mid-Pleistocene transition. *Sci. Adv.* **7:** eabj9341.

Zhang, F., S. Romaniello, Y. Cui, L. Zhao, Z.-Q. Chen, and A. Anbar. 2018. Congruent Permian-Triassic $\delta^{238}U$ records at Panthalassic and Tethyan sites: confirmation of global-oceanic anoxia and validation of the U-isotope paleoredox proxy. *Geology* **46:** 327–330.

Zhang, F., T. M. Lenton, Á. del Rey, S. J. Romaniello, X. Chen, N. J. Planavsky, M. O. Clarkson, T. W. Dahl, K. V. Lau, W. Wang *et al.* 2020. Uranium isotopes in marine carbonates as a global ocean paleoredox proxy: a critical review. *Geochim. Cosmochim. Acta* **287:** 27–49.